Three papers on inverse optimization algorithms, PEV sales forecasting, and PEVs' potential impact on power systems

by

Zhaoyang Duan

A dissertation submitted to the graduate faculty

in partial fulfillment of the requirements for the degree of

DOCTOR OF PHILOSOPHY

Major: Industrial Engineering

Program of Study Committee:

Lizhi Wang, Major Professor

Guiping Hu

Sarah Ryan

James McCalley

Mervyn Marasinghe

Iowa State University

Ames, Iowa

2014

DEDICATION

I would like to dedicate this dissertation to my parents Xiqi Duan, Yingzhen Su, and to my wife Yi Zou. Without their support I would not have been able to complete this work. I would also like to thank my friends for their help and guidance during the writing of this work.

TABLE OF CONTENTS

LIST OF TABLES

LIST OF FIGURES

ACKNOWLEDGEMENTS

I would like to take this opportunity to express my thanks to those who helped me with various aspects of conducting research and the writing of this thesis. First and foremost, I would like to thank my major professor Dr. Lizhi Wang, for his guidance, patience and support throughout this research and the writing of this thesis. His insights and words have encouraged me and his enthusiasm has inspired me to pursue a high level of research work. I would also appreciate my committee members for their efforts and contributions to this work: Dr. Sarah Ryan, Dr. Guiping Hu, Dr. James McCalley, and Dr. Mervyn Marasinghe. I would also like to thank my friends and family for their help during the writing of this work. Most of my graduate study has been supported by NETSCORE21 project, which should also be gratefully acknowledged.

ABSTRACT

This thesis consists of three journal papers that I have been worked on during my PhD program of study.

The first paper presents heuristic algorithms that are designed to be implemented and executed in parallel with an existing algorithm in order to overcome its two limitations. Computational experiments show that implementing the heuristic algorithm on one auxiliary processor in parallel with the existing algorithm on the main processor significantly improves its computational efficiency, in addition to providing a series of improving feasible upper bound solutions.

In the second paper, we present two interactive models to jointly forecast PEV sales and the diurnal recharging load curve in the U.S. between 2012 and 2020. A case study is conducted for the Midwest ISO region. Compared to the sales forecasts from the literature, our results turn out to be less optimistic. Our recharging load forecast results also suggest that, if appropriately managed, the impact of PEVs on electricity load would not be overwhelming in the next decade.

The third paper focuses on assessing and mitigating the potential impact of PEVs recharging load on power systems, Case study show that electricity rates with higher flexibility induces PEVs to have less impact on the power systems in terms of both generation cost and uncertainties. Also, PEV users higher recharging behavior responsiveness will improve the effectiveness of price incentives and the control ability of the power utilities under all types of TOU rates mechanisms.

CHAPTER 1. GENERAL INTRODUCTION

1.1 Introduction

A plug-in electric vehicle (PEV) is any motor vehicle that can be recharged from any external source of electricity. It includes all-electric vehicles and plug-in hybrid electric vehicles (PHEVs). Compared with conventional internal combustion engine vehicles, PEVs have the advantages of lower operating and maintenance costs, lower air pollution, lower green house gas emissions, and less dependence on imported oil. Several national governments have established tax credits and other incentives to promote the mass production of PEVs. The U.S. is one of the world's largest PEVs' markets as of December 2011. Since December 2010 when the first commercially available PEVs (Chevrolet Volt and Nissan Leaf) entered into the U.S. market, around 18,000 PEVs have been sold in the U.S. through December 2011.

Although PEV is regarded as possible solutions to the emissions and imported oil problems, it may cause new potential problems to the power systems. The ability to recharge batteries by plugging into an electric outlet extends the potential impacts of PEVs from transportation sector to the electric power systems sector. Unlike baseline electric load, PEV recharging load is much more instable. PEV users recharge their PEVs according to their convenience and availability without considering the burden of power systems under flat electricity rates. While for power systems, PEVs' recharging behaviors play a significant role in their impact on the power systems. The current power grid infrastructure has enough spare generating capacity to support a large PEV penetration level if most of recharging happens during off-peak load hours. Uncontrolled charging of PEVs may not only be much more costly to the power systems but also pose threat to the reliability and generation adequacy of the grid. As upper level

decision makers, power system operators manage to shift PEV recharging load to off-peak load hours through design of effective electricity rates. Moreover, sales of PEVs directly determines the magnitude of PEVs' potential impact on power systems. It is an important information to assess the long-term impact of PEVs, which could be dramatically more significant than foreseeable immediate impact.

In order to fully study the potential impact of PEVs on power systems, several related topics should be addressed. On one hand, an efficient measure should be established to assess the potential impact of PEV recharging load on power systems. We also need to design the optimal electricity rate mechanism which adjusts the PEV users' recharging behaviors to obtain the minimum impact on the power grid. In this process, PEV users' demand response model should also be built to study their load shift responses to the electricity rates. On the other hand, we also forecast PEVs sales and their diurnal recharging load for the next decade, which provide information for future impact prediction. Optimization and statistical methodologies will be mostly used in conducting our research.

Three papers are proposed in my dissertation. The first paper establishes heuristic algorithms for a type of optimization problem, which is named as inverse mixed integer linear programming problem. The second paper is to forecast PEVs sales and their diurnal recharging load curve using statistical and optimization methods. The last paper presents a way of measuring PEVs' potential impact on power systems, and it tries to design the optimal electricity rate plan which mitigates the potential impact under the PEV users' demand response model. These three papers have close relations. The first paper provides an efficient way of solving a particular type of problem which may be implemented in the last two papers. The last two papers cooperatively study the potential impact of PEVs on power systems and the ways of mitigating their impact.

The first paper is published in *Journal of Global Optimization* in November 2011. The second paper is published in *IEEE Transactions on Smart Grid* in January 2014. The following

three subsections are used to give a detailed introduction to each of the three papers.

1.1.1 Paper I: Heuristic Algorithms for the Inverse Mixed Integer Linear Programming Problem

The first paper presents heuristic algorithms that can be executed in parallel with an existing algorithm to improve its computational performance of solving the inverse mixed integer linear programming (InvMILP) problem. The InvMILP is a new extension to the well-studied inverse linear programming (InvLP) problem, which is to obtain the minimal perturbation to the objective function of a linear program (LP) in order to make a given solution optimal.

The recent development in inverse optimization, in particular the extension from the inverse linear programming problem to the inverse mixed integer linear programming problem, not only provides more powerful modeling tools but also presents more challenges to the design of efficient solution techniques. The only reported InvMILP algorithm, referred as $\text{Alg}^{\text{InvMILP}}$, although finitely converging to global optimality, suffers two limitations that greatly restrict its applicability: it is time consuming and does not generate a feasible solution except for the optimal one.

The heuristic algorithms presented in this paper are designed to be implemented and executed in parallel with $\text{Alg}^{\text{InvMILP}}$ in order to alleviate and overcome its two limitations. Computational experiments show that implementing the heuristic algorithm on one auxiliary processor in parallel with $\text{Alg}^{\text{InvMILP}}$ on the main processor significantly improves its computational efficiency, in addition to providing a series of improving feasible upper bound solutions. The additional speedup of parallel implementation on two or more auxiliary processors appears to be incremental, but the upper bound can be improved much faster.

1.1.2 Paper II: Forecasting Plug-in Electric Vehicles Sales and the Diurnal Recharging Load Curve

In the second paper, we present two interactive models to jointly forecast plug-in electric vehicles sales and the diurnal recharging load curve in the U.S.. The scope of our forecast is for the U.S. between 2011 and 2020, and PEVs include both plug-in hybrid electric vehicles (such as Chevrolet Volt) and pure electric vehicles (such as Nissan Leaf).

Our approach for PEV sales forecast is based on the observation that PEVs and HEVs share some key features, such as being more fuel efficient and expensive than conventional internal combustion engine vehicles (ICEVs), only to a varying extent. We first use a multiple linear regression model to extract the relationship between HEV sales and several explanatory factors from historical data, and then use a similar model to forecast PEV sales from estimated trajectories of the corresponding explanatory factors for PEVs. Our approach for diurnal recharging load forecast is based on our conjecture that PEV users' recharging behaviors will demonstrate a gradual transition from a convenience driven mode to a cost driven mode in the next decade.

The interactions between PEV sales forecast model and recharging load forecast model are bidirectional: PEV sales forecast helps determine the recharging profile and consequently the recharging cost, which then feeds back to the multiple linear regression model as part of an explanatory factor. When the two models have reached an equilibrium after iterations of interactions, we obtain our final forecast for both PEV sales and the diurnal recharging load.

A case study is conducted for the Midwest ISO region. Compared to the sales forecasts from the literature, our results turn out to be less optimistic. Our recharging load forecast results also suggest that, if appropriately managed, the impact of plug-in electric vehicles on electricity load would not be overwhelming in the next decade.

1.1.3 Paper III: Measuring and Mitigating Plug-in Electric Vehicles' Potential Impact on Power Systems

In the last paper, we focus on assessing the potential impact of PEVs recharging load on the power systems, and designing the optimal electricity rates that can effectively mitigate the impact of PEVs recharging load with consideration of PEV users' demand responses.

In this paper, we define two risk measures to represent both the cost magnitude and economic uncertainties that PEVs recharging load could bring to the power systems. Based on the defined risk measures, different electricity rate mechanisms are studied and compared, which include flat rates, 3-steps time of use (TOU) rates, and 24-steps TOU rates. Demand response is also incorporated to present how PEV users recharging behavior reacts to the electricity rate. The resulted optimal electricity rate mechanism is presented which has the lowest cost and brings smallest economic uncertainties to the power systems.

A 10-bus system case study is conducted. The optimal electricity rates under different rates mechanisms are designed and their performance are compared. The results show that 24-steps TOU rates has the best performance in terms of the two defined risk measures. It also shows how PEV users recharging behavior influences the risk measures. High recharging responsiveness increase the effectiveness of price incentives and the control ability of power utilities under all types of TOU rates mechanisms.

Multiple techniques, including optimization modeling, statistical analysis, Monte Carlo Simulation, are all applied in this paper. PEVs recharging loads are modeled as random variables, and risk measures are defined using concept of value at risk (VAR). Incorporating PEV users demand response into the study of PEVs impact on the power systems is also a key feature.

1.2 Thesis Organization

The remainder of this thesis is organized as follows. The three papers are presented in Chapter 2, 3, and 4, respectively. Contribution is in Chapter 5.

CHAPTER 2. HEURISTIC ALGORITHMS FOR THE INVERSE MIXED INTEGER LINEAR PROGRAMMING PROBLEM

A paper published in the *Journal of Global Optimization*

Zhaoyang Duan and Lizhi Wang

2.1 Introduction

This paper presents heuristic algorithms that can be executed in parallel with an existing algorithm to improve its computational performance of solving the inverse mixed integer linear programming (InvMILP) problem. The InvMILP is a new extension to the well-studied inverse linear programming (InvLP) problem, which is to obtain the minimal perturbation to the objective function of a linear program (LP) in order to make a given solution optimal. In [18], the InvLP is extended to InvMILP, which allows the lower level optimization to be a mixed integer linear program (MILP). The resulting InvMILP formulation is significantly more complex than InvLP, and the only reported solution technique is the cutting plane algorithm, referred to as $\text{Alg}^{\text{InvMILP}}$ in [18]. However, this algorithm suffers two prominent limitations: it may require solving a large number of MILPs and it does not yield a feasible solution until the terminating iteration. The heuristic algorithms presented in this paper are designed to alleviate and overcome these two limitations.

The literature on inverse optimization has mainly focused on InvLP. Burton et al. [6] study inverse shortest path problems, which have been used in predicting earthquakes. Zhang et al. [21] formulate an inverse shortest path problem as an LP and propose a column generation method for the problem. The inverse maximum capacity path problem is studied in [19].

Ahuja et al. [2] present an LP formulation of the InvLP and show in general that as long as the optimization problem has a linear cost function and is polynomially solvable, its inverse problems are also polynomially solvable under the weighted L_1 and L_∞ norms. Since the late 1980s, inverse optimization has been applied to a wide variety of applications, such as geophysics [14, 15, 16], traffic control [8, 9], high-speed networks [10], aircraft design [13], auction design [4], plant location [5], and healthcare [12].

Wang [18] extends InvLP to InvMILP, which is to find a minimal perturbation Δc, measured by some norm $||\Delta c||$, such that a given target solution x^t becomes optimal to the MILP

$$\max_x \left\{ (c + \Delta c)^\top x : Ax \leq b, x \geq 0, x^I \in \mathbb{Z}^{|I|} \right\},$$

where $A \in \mathbb{R}^{m \times n}$, $b \in \mathbb{R}^m$, $c \in \mathbb{R}^n$, and $I \subseteq \{1, ..., n\}$. We will use $\mathcal{IP}(A, b, c, I)$ and $\mathcal{LP}(A, b, c)$ to denote the MILP $\max_x\{c^\top x : Ax \leq b, x \geq 0, x_I \in \mathbb{Z}\}$ and its LP relaxation $\max_x\{c^\top x : Ax \leq b, x \geq 0\}$, respectively. We shall assume that x^t is feasible to $\mathcal{IP}(A, b, c, I)$, otherwise the InvMILP is simply infeasible. The InvMILP can be formulated as

$$\min_{\Delta c} \quad ||\Delta c|| \tag{2.1}$$

$$\text{s.t.} \quad x^t \in \text{argmax}_x \left\{ (c + \Delta c)^\top x : Ax \leq b, x \geq 0, x^I \in \mathbb{Z}^{|I|} \right\}. \tag{2.2}$$

The extension from InvLP to InvMILP has important practical applications such as designing effective incentive policies for promoting renewable energy. Power systems are largely cost-minimization oriented [3, 17], thus government incentive policy (subsidies and tax credits) intervention is indispensable for achieving a more renewable energy portfolio. The problem of using minimal amount of subsidies and tax credits to stimulate a higher level of investment in new renewable generation is therefore naturally an inverse optimization problem. The inherently discrete nature of investment decisions requires that both discrete and continuous variables be considered in the lower level optimization.

In this paper, we focus our discussion on InvMILP under the weighted L_1 norm, thus $||\Delta c||$ becomes $w^\top |\Delta c|$, where $w \in \mathbb{R}^n_+$ is a constant vector. As Heuberger [11] points out, a

polynomial-time InvMILP algorithm does not exist unless *co*-$\mathcal{NP} = \mathcal{NP}$. The cutting plane algorithm $\text{Alg}^{\text{InvMILP}}$ presented in [18] is the only InvMILP solution technique that we are aware of. Although it is proved to be finitely converging to global optimality, it is time consuming to solve the inverse problems of even small-sized MILPs. Moreover, the algorithm does not generate any feasible solution except for the optimal one in the terminating iteration. Motivated by the complexity of the problem and the limitations of the algorithm, we present heuristic algorithms to improve the computational performance of $\text{Alg}^{\text{InvMILP}}$. The heuristic algorithms are designed to be executed on one or multiple auxiliary processors in parallel with $\text{Alg}^{\text{InvMILP}}$. We also test the potential improvement as a function of the number of auxiliary processors.

The remainder of this paper is organized as follows. In Section 2.2, we review the cutting plane algorithm $\text{Alg}^{\text{InvMILP}}$. In Section 3.2, we present the heuristic algorithms for one and multiple auxiliary processors. Computational experiment results are reported in Section 3.3. Section 3.4 concludes the paper.

2.2 The Existing InvMILP Algorithm

In this section, we briefly review the cutting plane algorithm $\text{Alg}^{\text{InvMILP}}$ presented in [18]. If we define $e, f \in \mathbb{R}^n_+$ such that $\Delta c = e - f$, then the objective function (2.1) under the weighted L_1 norm can be replaced with $w^\top e + w^\top f$. The $\text{Alg}^{\text{InvMILP}}$ consists of the following three steps:

Step 0 Initiate $\mathcal{S}^0 = \emptyset$.

Step 1 Solve the following LP and let (y^L, e^L, f^L) be an optimal solution.

$$\min_{y,e,f} \quad w^\top e + w^\top f \tag{2.3}$$

$$\text{s.t.} \quad A^\top y \geq c + e - f \tag{2.4}$$

$$(c + e - f)^\top x^t \geq (c + e - f)^\top x^0, \quad \forall x^0 \in \mathcal{S}^0 \tag{2.5}$$

$$y, e, f \geq 0. \tag{2.6}$$

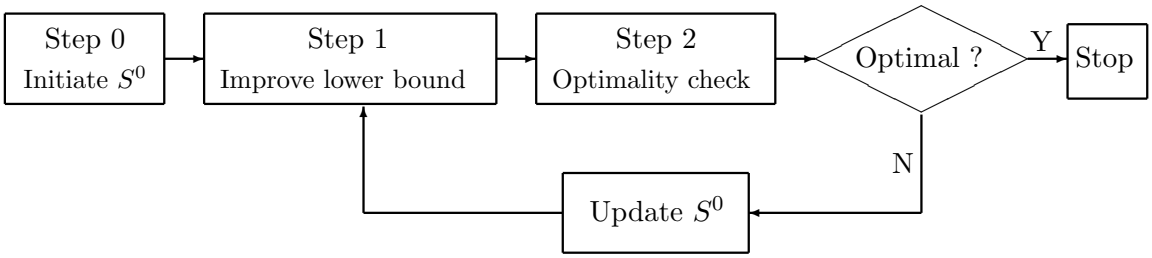

Figure 2.1 Diagram of the algorithm $\text{Alg}^{\text{InvMILP}}$

Step 2 Let x^0 be an optimal solution to $\mathcal{IP}(A, b, c + e^L - f^L, I)$. If $(c + e^L - f^L)^\top x^t \geq (c + e^L - f^L)^\top x^0$, then stop, and $\Delta c^L = e^L - f^L$ is optimal to InvMILP (2.1)-(2.2). Otherwise update $\mathcal{S}^0 = \mathcal{S}^0 \cup \{x^0\}$ and go back to Step 1.

In Step 0, the set of known extreme points of the convex hull of $\{Ax \leq b, x \geq 0, x_I \in \mathbb{Z}^{|I|}\}$, $\mathcal{S}^0$, is initiated, which will be updated as new extreme points are discovered. Step 1 generates a lower bound solution $\Delta c^L = e^L - f^L$ that has minimized norm but may or may not make x^t optimal. Therefore, Step 2 checks the optimality of x^t with respect to $\mathcal{IP}(A, b, c + \Delta c^L, I)$. If the answer is positive, then Δc^L is proved to be optimal to (2.1)-(2.2); otherwise a new extreme point x^0 is generated and added to the set $\mathcal{S}^0$. The Step 1 – Step 2 loop continues until the optimality of x^t is confirmed in Step 2. The process of the cutting plane algorithm for InvMILP is illustrated in Figure 2.1.

Theorem[**18**]: Algorithm $\text{Alg}^{\text{InvMILP}}$ terminates finitely with an optimal solution to (2.1)-(2.2).

Two prominent limitations of the cutting plane algorithm are mentioned in [18]. First, an MILP needs to be solved in every iteration and the algorithm may take many iterations to terminate. This is because only one new extreme point is discovered in Step 1, and the number of extreme points in $\mathcal{S}^0$ that are necessary to ensure the optimality of x^t with respect to $\mathcal{IP}(A, b, c + e^L - f^L, I)$ could be large, although it need not be equal to the total number of extreme points of the convex hull of $\{Ax \leq b, x \geq 0, x_I \in \mathbb{Z}^{|I|}\}$. Second, the solution

$\Delta c^L = e^L - f^L$ from Step 1 is infeasible to (2.1)-(2.2) until the terminating iteration, thus the algorithm does not allow the tradeoff between reduced computation time and compromised solution quality. Considering the complexity of the InvMILP problem, these limitations restrict the applicability of the algorithm from practical problems with larger dimensions.

2.3 Parallel Add-on Heuristic Algorithms

Motivated by the limitations of $\text{Alg}^{\text{InvMILP}}$, we present in this section heuristic algorithms that can be implemented and executed in parallel with $\text{Alg}^{\text{InvMILP}}$ to alleviate and overcome these limitations. We first introduce the algorithm for one auxiliary processor, and then extend it to multiple auxiliary processors.

2.3.1 Parallel Add-on Heuristic Algorithm for One Auxiliary Processor

If one auxiliary processor is available for computation and communication with the main processor on which the $\text{Alg}^{\text{InvMILP}}$ is implemented and executed, then the following heuristic algorithm, which will be referred to as $\text{PAlg}^{\text{InvMILP}}$, can be used to reduce the number of iterations and to compute an improving upper bound. To concurrently execute $\text{Alg}^{\text{InvMILP}}$ with this heuristic algorithm, the set $\mathcal{S}^0$ and the lower bound solution Δc^L both need to be stored on shared memory so that they can be continuously written and read by all processors.

Algorithm $\text{PAlg}^{\text{InvMILP}}$ for InvMILP (2.1)-(2.2)

Step A Solve the following LP.

$$\min_{y,e,f} \quad w^\top e + w^\top f \tag{2.7}$$

$$\text{s.t.} \quad A^\top y \geq c + e - f \tag{2.8}$$

$$b^\top y = (c + e - f)^\top x^t \tag{2.9}$$

$$y, e, f \geq 0. \tag{2.10}$$

Let (y^U, e^U, f^U) be an optimal solution. Then $\Delta c^U = c + e^U - f^U$ is an initial upper bound solution to InvMILP (2.1)-(2.2).

Step B Define $g = w^\top(|\Delta c^U| - |\Delta c^L|)$ as the gap between the current upper bound Δc^U and the most updated lower bound Δc^L from Step 1 of $\text{Alg}^{\text{InvMILP}}$. Try to reduce this gap by $\theta \in (0,1)$ by solving the following LP and let (y^1, e^1, f^1, s^1) be an optimal solution.

$$\max_{y,e,f,s} \quad s \tag{2.11}$$

$$\text{s.t.} \quad w^\top e + w^\top f \le w^\top e^L + w^\top f^L + (1-\theta)g \tag{2.12}$$

$$A^\top y \ge c + e - f \tag{2.13}$$

$$(c+e-f)^\top x^t \ge (c+e-f)^\top x^0 + s, \quad \forall x^0 \in \mathcal{S}^0 \tag{2.14}$$

$$y, e, f, s \ge 0 \tag{2.15}$$

Step C Let x^1 be an optimal solution to $\mathcal{IP}(A, b, c + e^1 - f^1, I)$. If $(c + e^1 - f^1)^\top x^t \ge (c + e^1 - f^1)^\top x^1$, then update the upper bound solution $\Delta c^U = c + e^1 - f^1$; otherwise update $\mathcal{S}^0 = \mathcal{S}^0 \cup \{x^1\}$. Go back to Step B.

We interpret this algorithm as follows. In Step A, (2.7)-(2.10) solves the InvLP for $\mathcal{LP}(A, b, c)$ [18]. The optimal solution $\Delta c^U = c + e^U - f^U$ provides an initial upper bound to InvMILP (2.1)-(2.2), since x^t is optimal to $\mathcal{LP}(A, b, c + \Delta c^U)$ implies that it is also optimal to $\mathcal{IP}(A, b, c + \Delta c^U, I)$ as long as x^t is feasible to $\mathcal{IP}(A, b, c, I)$. In Step B, we heuristically improve the upper bound Δc^U by trying to reduce the gap between upper and lower bounds by θ (in percentage), as required in Constraint (2.12). At the same time, we also attempt to maintain the optimality of x^t by maximizing s, defined in Constraint (2.14), which represents the superiority of x^t over other extreme points in $\mathcal{S}^0$. Step C checks the optimality of the target solution x^t to $\mathcal{IP}(A, b, c + \Delta c^1, I)$. If x^t remains optimal, then Δc^1 is an improved upper bound solution; otherwise we will update $\mathcal{S}^0$ to include the newly discovered extreme point x^1. Therefore, each iteration of $\text{PAlg}^{\text{InvMILP}}$ either helps $\text{Alg}^{\text{InvMILP}}$ to add another new extreme point solution into $\mathcal{S}^0$, alleviating the first limitation of $\text{Alg}^{\text{InvMILP}}$, or improves the upper

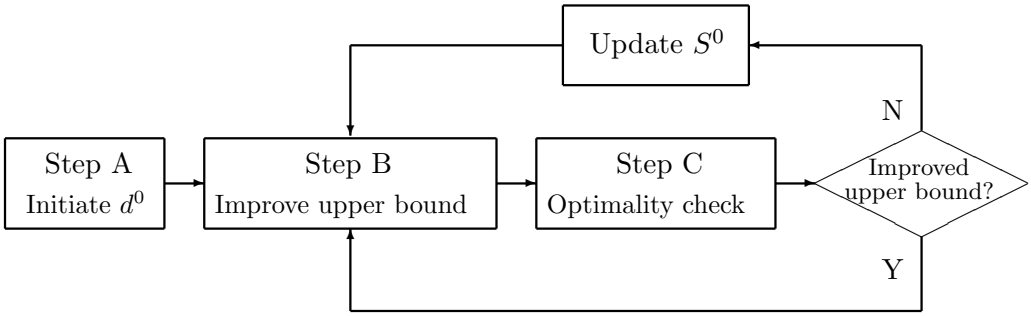

Figure 2.2 Diagram of $\text{PAlg}^{\text{InvMILP}}$

bound, overcoming the second limitation. This algorithm will continue to go through the Step B – Step C loop until $\text{Alg}^{\text{InvMILP}}$ has found the optimal solution, and then $\text{PAlg}^{\text{InvMILP}}$ will be terminated externally. Different values of parameter θ could lead to different performances of $\text{PAlg}^{\text{InvMILP}}$. A larger value of θ tends to generate more new extreme points and update the upper bound less often since it tries to close the gap too fast; on the other hand, a smaller value of θ only tries to slowly close the gap thus is more likely to find improved upper bounds and generate less new extreme points. The process of $\text{PAlg}^{\text{InvMILP}}$ is illustrated in Figure 2.2.

2.3.2 Parallel Add-on Heuristic Algorithms for Multiple Auxiliary Processors

It is a natural extension to apply similar algorithms for multiple auxiliary processors to further improve the computational efficiency. For the one auxiliary processor case, each iteration either helps $\text{Alg}^{\text{InvMILP}}$ to add a new extreme point to $\mathcal{S}^0$ or improves the upper bound, thus in theory no computation effort is wasted. For the multiple auxiliary processors case, however, special effort should be made to minimize the possibility that the upper bound solutions Δc^U generated in Step B of different auxiliary processors result in the same extreme point x^0, in which case the effect of multiple auxiliary processors is reduced to be the same as one auxiliary processor. For that purpose, we choose different values of parameters w and θ in Constraint (2.12) for different auxiliary processors. For example, $w = [100, 1, 100, 1, ...]^\top$ with $\theta = 0.8$ and $w = [1, 100, 1, 100, ...]^\top$ with $\theta = 0.2$ will tend to lead to distinct perturbation directions Δc^1, which will hopefully generate different extreme points in order to reduce redundant computa-

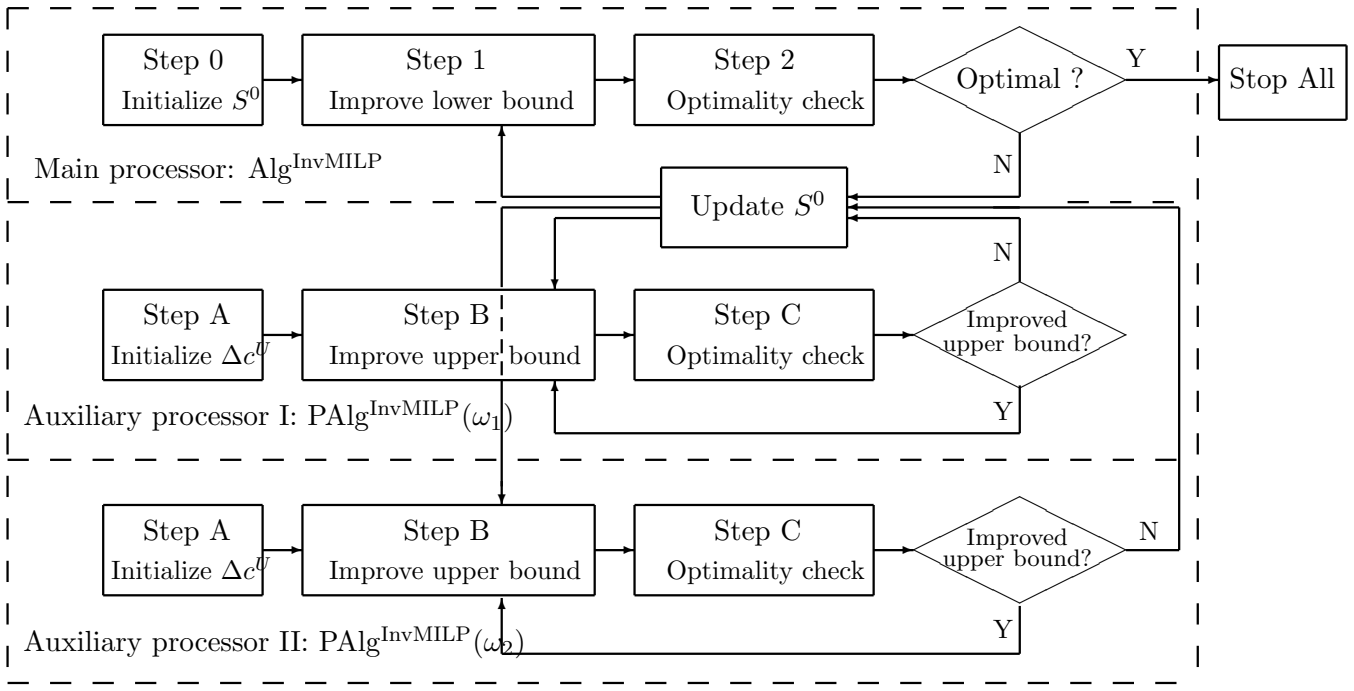

Figure 2.3 Diagram of $\text{PAlg}^{\text{InvMILP}}$ on two auxiliary processors in parallel with $\text{Alg}^{\text{InvMILP}}$ on the main processor

tion effort. The process of executing $\text{Alg}^{\text{InvMILP}}$ on the main processor and $\text{PAlg}^{\text{InvMILP}}$ on two auxiliary processors is illustrated in Figure 2.3 as an example.

2.4 Computational Experiments

In this section, we test the speedup of the parallel implementation on a group of MILP instances from the mixed integer problem library (MIPLIB) [1] as well as 4 randomly generated ones. The random instances are named `MILP15`, `MILP20`, `MILP30`, and `MILP50`, with the dimensions ($n = m$) indicated after '`MILP`'. For each instance, we use randomly generated objective functions to obtain up to 50 different optimal solutions, which will be used as target solutions x^t. We then solve the inverse problem of all instances for all the optimal solutions. Computational results in Tables 2.1 and 2.2 are all average values of 50 instances. All the algorithms are implemented in MATLAB using TOMLAB/CPLEX as the MILP solver on a network of computers each with a 3.25 GB ram and a 3.00 GHz CPU.

Table 2.1 Sequential implementation results

MILP	# auxiliary processors					
	0	1	2	3	4	5
	# iter.	# iter.	# iter.	# iter.	# iter.	# iter.
egout	27.9	14.9	12.4	10.7	9.9	9.5
gt2	96.2	57.6	56.7	42.0	41.0	39.2
mode008	18.0	10.7	10.0	8.7	8.5	7.8
lseu	62.3	41.6	38.9	36.1	35.8	31.7
p0201	70.0	47.6	41.8	40.8	34.9	33.3
p0033	12.2	7.5	7.1	6.1	5.5	5.5
stein27	39.3	21.5	19.8	18.4	15.5	14.3
stein45	57.9	33.6	32.0	29.5	25.2	23.4
flugpl	7.4	5.1	4.8	4.5	4.6	3.9
p0282	109.1	91.7	92.5	81.4	76	72.7
bell5	800.2	695.8	686.3	709.1	669.8	635.8
rgn	493.2	248	241.3	238.9	247.6	221.7
MILP15	28.6	13.2	11.8	11.1	11.0	9.9
MILP20	50.8	29.7	26.3	22.3	21.8	20.7
MILP30	123.8	70.9	85.7	81.6	69.6	61.2
MILP50	161.8	121.2	111.7	109.1	93.0	84.7

To test the extent to which parallel implementation of $\text{PAlg}^{\text{InvMILP}}$ on multiple auxiliary processors could potentially speed up $\text{Alg}^{\text{InvMILP}}$, we first execute the tasks of multiple processors on one processor in a sequential manner. Assuming that the loops of Step 1-Step 2 on the main processor and Step B-Step C on the auxiliary processors are approximately synchronized, we use the number of iterations of the sequential implementation as an estimate of that of the parallel implementation. Table 2.1 shows the number of iterations to solve the inverse problem of 16 MILP instances, of which 12 are from MIPLIB and 4 are randomly generated. Compared to the benchmark case with only the main processor and no auxiliary ones, the addition of $\text{PAlg}^{\text{InvMILP}}$ on multiple auxiliary processors reduces the number of iterations, but the marginal improvement has a sudden decrease as the number of auxiliary processors exceeds one.

Informed by the result from Table 2.1, we decided to only implement $\text{PAlg}^{\text{InvMILP}}$ on one and two auxiliary processors to test the actual speedup that we can achieve. The computational results for the one and two auxiliary processors are shown in Table 2.2. For the

former case, the parameters are $w = [1, 1, ..., 1]$; for the latter case, $w_1 = [1, 1, ..., 1]$ and $w_2 = [100, 1, 100, 1, ..., 100, 1]$. $\theta = 0.8$ is used for both cases to put more weight on generating more extreme points.

The results in Table 2.2 show that parallel implementation on one and two auxiliary processors reduces the number of iterations to a discounted extent compared to the sequential implementation. The percentage of computation time improvement is also smaller than that of the number of iterations. This is largely due to the frequent communications between the main and auxiliary processors that are necessary to implement the algorithms.

We emphasize here that reducing the number of iterations and computation time is only one goal of $\text{PAlg}^{\text{InvMILP}}$, and the other goal is to provide a series of improving feasible upper bound solutions. The effectiveness of $\text{PAlg}^{\text{InvMILP}}$ in achieving the latter goal is illustrated in Fig. 2.4 for the instance `stein27` as an example. The flat dotted line is the optimal objective value; the bottom curve shows how a series of improving lower bound solutions generated from $\text{Alg}^{\text{InvMILP}}$ approach the optimal value iteratively; and the two curves on top are the two series of improving feasible upper bound solutions generated from $\text{PAlg}^{\text{InvMILP}}$ on the one and two auxiliary processors. The upper bound from two auxiliary processors approaches the optimal value much faster than that from one auxiliary processor, which justifies the uses of multiple auxiliary processors, especially when obtaining a good feasible solution within a reasonable time period is more important than the certificate of optimality.

2.5 Conclusion

The InvMILP is intrinsically hard to solve and $\text{Alg}^{\text{InvMILP}}$ is the only reported algorithm that we are aware of. The heuristic algorithms presented in this paper are designed to improve the computational performances of $\text{Alg}^{\text{InvMILP}}$. On the one hand, it reduces the time and number of iterations for $\text{Alg}^{\text{InvMILP}}$ to terminate; on the other hand, it also yields a series of improving feasible upper bound solutions that allow the tradeoff between reduced computation

Table 2.2 Parallel implementation results for $\text{Alg}^{\text{InvMILP}}$ and $\text{PAlg}^{\text{InvMILP}}$ on one and two auxiliary processors

MILP	$\text{Alg}^{\text{InvMILP}}$		+ $\text{PAlg}^{\text{InvMILP}}$		improvement		+ 2×$\text{PAlg}^{\text{InvMILP}}$		improvement	
	# iter.	# sec.	# iter.	# sec.	# iter.	# sec.	# iter.	# sec.	# iter.	# sec.
egout	27.9	10.7	20.5	7.3	26.5%	31.8%	19.5	5.9	30.1%	44.9%
gt2	96.2	49.3	65.7	40.7	31.7%	17.4%	77.8	38.2	19.1%	22.5%
mod008	18.0	11.9	15.3	11.0	15.0%	7.6%	14.7	8.8	18.3%	26.1%
lseu	62.3	23.5	49.5	19.7	20.5%	16.2%	53.2	18.6	14.6%	20.9%
p0201	70.0	37.3	55.9	34.0	20.1%	8.8%	56.5	28.7	19.3%	23.1%
p0033	12.2	2.7	11.5	2.6	5.7%	3.7%	9.9	2.6	18.9%	3.7 %
stein27	39.3	19.4	30.4	12.6	22.6%	35.1%	29.6	11.4	24.7%	41.2%
stein45	57.9	177.0	33.6	119.7	42.0%	32.4%	32.9	108.1	43.2%	38.9%
flugpl	7.4	2.7	7.1	1.5	4.1%	44.4%	6.7	2.3	9.5%	14.8%
p0282	109.1	98.0	99.14	88.7	9.1%	9.5%	95.6	93.1	12.4%	5.0%
bell5	800.2	506.0	772.3	750.2	3.5%	-48.3%	732.6	670.8	8.4%	-32.6%
rgn	493.2	300.2	360.8	341.0	26.8%	-13.6%	317.1	253.2	35.7%	-15.7%
MILP15	28.6	11.6	22.9	8.4	19.9%	27.6%	22.4	6.2	21.7%	46.6%
MILP20	50.8	22.5	39.1	16.6	23.0%	26.2%	39.1	15.4	23.0%	31.6%
MILP30	123.8	78.0	102.5	76.7	17.2%	1.7%	103.8	58.4	16.2%	25.1%
MILP50	161.8	508.8	126.6	487.6	21.8%	4.2%	118.9	355.3	26.5%	30.2%
				average	19.4%	12.8%		average	21.4%	20.4%

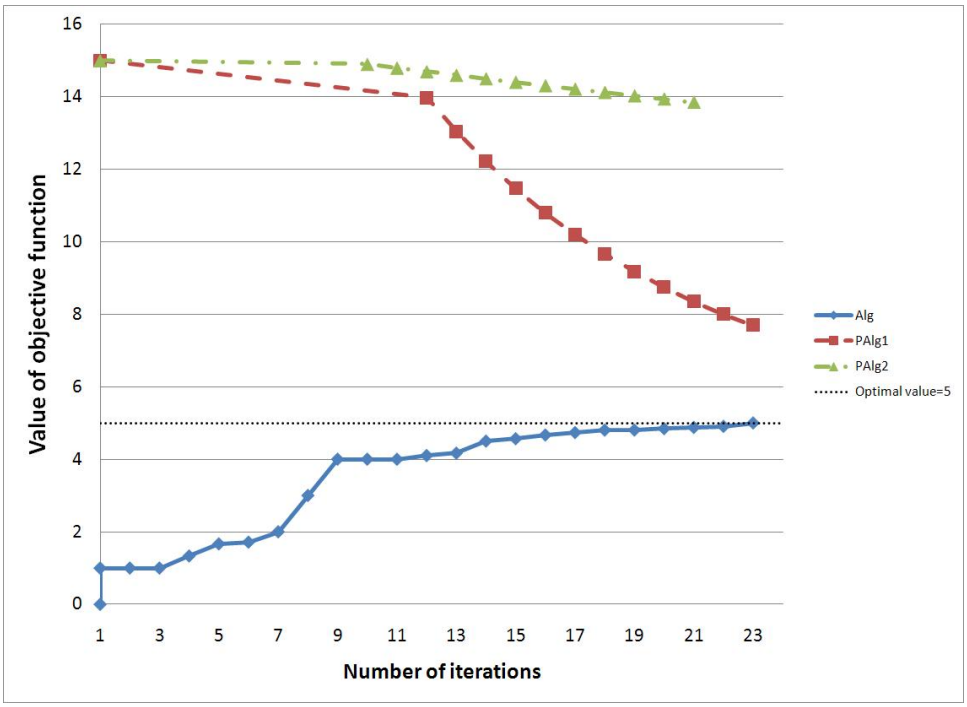

Figure 2.4 Lower and upper bounds generated from $\text{Alg}^{\text{InvMILP}}$ and $\text{PAlg}^{\text{InvMILP}}$ for instance `stein27`

time and compromised solution quality.

Computational experiments on MIPLIB instances as well as randomly generated ones suggest that, when implemented in parallel on an auxiliary processor, $\text{PAlg}^{\text{InvMILP}}$ is able to significantly speedup $\text{Alg}^{\text{InvMILP}}$. The additional speedup using more auxiliary processors appears to be less than linear. This is largely caused by the possibility that multiple auxiliary processors generate a same new extreme point thus not make the contribution proportional to the number of processors. The feasible upper bound generated from multiple auxiliary processors, however, approaches to the optimal solution much faster than that from a single auxiliary processor.

Despite their limitations, the heuristic algorithms make a distinct contribution to the literature by demonstrating the potential effectiveness in alleviating and overcoming the two limitations of the only InvMILP algorithm using high-performance computing facilities. The InvMILP is intrinsically much harder than regular $\mathcal{NP}$-hard MILP, since even checking the feasibility of a solution Δc to the InvMILP (2.1)-(2.2) is $\mathcal{NP}$-hard. Such enormous complexity suggests that a polynomial-time InvMILP algorithm is extremely unlikely to exist, thus designing heuristic algorithms that could improve the computational efficiency and generate good feasible solutions in a timely manner becomes an important research topic.

Future research directions include designing more effective strategies to differentiate the searching directions of different auxiliary processors, improving communication efficiency of the parallel implementation, and exploring special heuristics for problems with special structures.

Bibliography

[1] T. Achterberg and T. Koch and A. Martin, "MIPLIB 2003," *Operations Research Letters*, 34, 361-372 (2006)

[2] R.K. Ahuja and J.B. Orlin, "Inverse optimization," *Operations Research*, 49, 771-783 (2001)

[3] S. Awerbuch, "Portfolio-based electricity generation planning: policy implications for renewables and energy security," *Mitigation and Adaptation Strategies for Global Change*, 11, 693-710 (2006)

[4] D.R. Beil and L.M. Wein, "An inverse-optimization-based auction mechanism to support a multiattribute RFQ process," *Management Science*, 49, 1529-1545 (2003)

[5] G.R. Bitran and V. Chandru and D.E. Sempolinski and J.F. Shapiro, "Inverse optimization: an application to the capacitated plant location problem," *Management Science*, 27, 1120-1141 (1981)

[6] D. Burton and Ph.L. Toint, "On an instance of the inverse shortest paths problem," *Mathematical Programming*, 53, 45-61 (1992)

[7] M.C. Cai and X.G. Yang and J.Z. Zhang, "The complexity analysis of the inverse center location problem," *Journal of Global Optimization*, 15, 213-218 (1999)

[8] R.B. Dial, "Minimal-revenue congestion pricing part I: A fast algorithm for the single-origin case," *Transportation Research Part B*, 33, 189-202 (1999)

[9] R.B. Dial, "Minimal-revenue congestion pricing part II: An efficient algorithm for the general case," *Transportation Research Part B*, 34, 645-665 (2000)

[10] A. Faragó and Á. Szentesi and B. Szviatovszki, "Inverse optimization in high-speed networks," *Discrete Applied Mathematics*, 129, 83-98 (2003)

[11] C. Heuberger, "Inverse combinatorial optimization: a survey on problems, methods, and results," *Journal of Combinatorial Optimization*, 8, 329-361 (2004)

[12] C.W. Hurkmans and G.J. Meijer and C. van Vliet-Vroegindeweij and M.J. van der Sangen and J. Cassee, "High-dose simultaneously integrated breast boost using intensity-modulated radiotherapy and inverse optimization," *International Journal of Radiation Oncology Biology Physics*, 66, 923-930 (2006)

[13] H. Kim and O. Rho, "Dual-point design of transonic airfoils using the hybrid inverse optimization method," *Journal of Aircraft*, 34, 612-618 (1997)

[14] W. Menke, "Geophysical data analysis: discrete inverse theory," Academic Press, San Diego (1989)

[15] T.J. Moser, "Shortest paths calculation of seismic rays," *Geophysics*, 56, 59-67 (1991)

[16] A. Tarantola, "Inverse problem theory: methods for data fitting and model parameter estimation," Elsevier, Amsterdam (1987)

[17] L. Wang and M. Mazumdar, "Using a system model to decompose the effects of influential factors on locational marginal prices," *IEEE Transactions on Power Systems*, 22, 1456-1465 (2007)

[18] L. Wang, "Cutting plane algorithms for the inverse mixed integer linear programming problem," *Operations Research Letters*, 37, 114-117 (2009)

[19] C. Yang and J. Zhang, "Two general methods for inverse optimization problems," *Applied Mathematics Letters*, 12, 69-72 (1999)

[20] B. Zhang and J. Zhang and Y. He, "Constrained inverse minimum spanning tree problems under the bottleneck-type Hamming distance," *Journal of Global Optimization*, 34, 467-474 (2006)

[21] J. Zhang and Z. Ma and C. Yang, "A column generation method for inverse shortest path problems," *Mathematical Methods of Operations Research*, 41, 347-358 (1995)

CHAPTER 3. FORECASTING PLUG-IN ELECTRIC VEHICLES SALES AND THE DIURNAL RECHARGING LOAD CURVE

A paper published in the *IEEE Transactions on Smart Grid*

Zhaoyang Duan, Brittni Gutierrez, and Lizhi Wang

3.1 Introduction

Whereas plug-in electric vehicles (PEVs) have been identified by many as part of a solution to problems in the transportation sector, the electric power systems must be prepared to embrace the new challenges and opportunities that come with the recharging load. Numerous studies [8, 18, 20, 19, 24, 25, 35, 37, 39, 23] have been conducted to assess the potential impact of PEVs on electric power systems, but many are based on two simplifying assumptions with insufficient justifications: the number of PEVs on the road and the fleet's diurnal recharging load curve. However, these assumptions have critical implications: the former is a direct multiplier of the magnitude of impact, and the latter affects the cost of serving the recharging load. Moreover, these two assumptions are also interdependent: on the one hand, the recharging load of a small number of PEVs may be buried in the fluctuation of the baseline load (electricity load other than PEV recharging load), whereas a proliferated fleet could overwhelm the generation capacity during peak load hours; on the other hand, PEV sales will also be affected by the availability of recharging infrastructures, including smarter electric rates and meters, which also influence PEV recharging load. In this paper, we propose a new approach to forecasting PEV sales and the diurnal recharging load, which incorporates their interdependencies.

Lack of precedent information is one of the largest challenges that the proposed forecasting task faces. The world's first mass produced PEVs, BYD F3DM, were sold to the general public in China in March 2010; Chevrolet Volt and Nissan Leaf both debuted in the U.S. market in late 2010. For many early adopters, power outlets in home garages are likely the primary recharging facilities in the near term, but many emerging technologies and business models that are under rapid development may also reshape people's recharging behavior in the longer term. What further complicates the forecasting task is the various factors that jointly influence the dynamics of PEV sales and the recharging load but are themselves hard to predict, such as gas prices, electric rates, recharging infrastructures, vehicle prices, and government incentives.

Despite the many challenges, forecast information of PEV sales and the recharging load is urgently needed to assess PEVs' longer-term implications on power systems, which could be dramatically more significant than the immediate impact that has been unnoticeable heretofore. Several existing studies have addressed these issues. A Pacific Northwest National Laboratory (PNNL) study [6] examines PEV market penetration scenarios based on information obtained from the literature and interviews with industry representatives as well as technical experts. Annual market penetration rates for PEVs are forecast from 2013 through 2045 for three scenarios: hybrid technology-based assessment, R&D goals achieved, and supply constrained scenarios, in which PEV market penetration is forecast to reach 9.7%, 9.9%, and 26.9% by 2023, and 11.9%, 29.8%, and 72.7% by 2045, respectively. An Electric Power Research Institute (EPRI) report [3] forecasts new vehicle market shares of conventional, hybrid, and plug-in electric vehicles using choice based market modeling of customer preference. Its results show that PEVs will have a market share of 20%, 62%, and 80% by 2050 in the low, medium and high penetration scenarios, respectively. An Oak Ridge National Laboratory (ORNL) study [19] estimates that the demand of PEVs will be approximately 1 million by 2015, which concurs with President Obama's expectation of 1 million PEVs on the road by 2015. ORNL's Market Acceptance of Advanced Automotive Technologies Model and UMTRI's Virtual Automotive Marketplace Model are used to assess a list of policy options in terms of their potential for boosting PEV sales in the next couple of decades. In a Morgan Stanley report [4], proprietary

information is used to forecast sales of hybrid electric vehicles and PEVs. Their forecast is that market demand will reach 250,000 by 2015 and 1 million by 2020. In a related study, Gallagher et al. [15] used a multiple linear regression model to estimate how hybrid electric vehicle sales respond to various types of incentives. Their empirical results show that "a one thousand dollar tax waiver is associated with a 45% increase in hybrid vehicle sales, whereas a one thousand dollar income tax credit is associated with a 3% increase in hybrid vehicle sales." They also estimated the implicit discount rate by comparing consumers' relative weights of upfront cost and future energy costs when deciding between hybrid electric vehicles (HEVs) and conventional vehicles. An implicit discount rate of 28.9% was reported for an eight-year vehicle lifespan. Other recognized market predictions of PEVs also include [36, 1, 4].

The shape of the diurnal recharging load curve of a PEV fleet is largely driven by two main forces: convenience and cost. On the one hand, PEV users would only plug in when their vehicles are parked close to an electric outlet for a long period of time, which in the short term is most likely to take place in their home garage from evening to next morning, but could extend to other locations and hours depending on individual users' driving habits and the development of recharging infrastructures. On the other hand, power systems have a strong preference for PEVs to avoid recharging during peak hours of the baseline load, because it would not only be much more costly to serve the additional electricity load but also pose threat to the reliability and generation adequacy of the grid. If PEV users face flat electric rates, which applied to 95% of U.S. homes and businesses in 2009 [8], then their recharging behaviors would be solely determined by the convenience factor; if their PEV load is charged at smarter electric rates that reflect actual real-time cost of serving the recharging load, then the cost factor would also play an important role in shaping the fleet's diurnal recharging load curve. Most existing studies on the PEV recharging load are based on the tradeoff between these two factors. In the EPRI study [3], it is assumed that 74% of the recharging energy is delivered from 10 PM to 6 AM, and the remaining 26% in the rest of the day. Clement-Nyns et al. [7] compared uncoordinated and coordinated recharging scenarios. In the uncoordinated case, convenience is the only driving force of the PEV load; in the coordinated case, they use a stochastic pro-

gramming approach to determine the optimal recharging profile in order to minimize the power losses and maximize the main grid load factor. Wang et al. [23] studied the potential impact of six different PEV recharging profiles on locational marginal prices: daytime (8 AM to 7 PM), nighttime (8 PM to 7 AM), decentralized and centralized (both with and without vehicle-to-grid) recharging profiles. In the decentralized recharging scenario, PEV users are assumed to choose six hours in each day with lowest electric rates to plug in. In the centralized recharging scenario, a battery station owner provides hot-swap services to PEV users and chooses the cheapest hours of the day to recharge a large number of batteries. In both scenarios, vehicle-to-grid technology is considered as an option for PEVs to discharge power back to the grid when electric rates are high. Elgowainy et al. [12] studied the impacts of charging choices for PEVs in 2030 and concluded that "the marginal-generation mixes produced 40% to 45% lower GHG emissions by PHEVs than did conventional gasoline internal combustion engine vehicles."

In this paper, we present two interactive models that jointly forecast PEV sales and the diurnal recharging load. The scope of our forecast is for the U.S. between 2012 and 2020, and PEVs include both plug-in hybrid electric vehicles (such as Chevrolet Volt) and pure electric vehicles (such as Nissan Leaf). Our approach for PEV sales forecast is based on the observation that PEVs and HEVs share some key features, such as being more fuel efficient and having a higher price tag than conventional internal combustion engine vehicles (ICEVs), only to a varying extent. We first use a multiple linear regression model to extract the relationship between HEV sales and several explanatory factors from historical data, and then use a similar model to forecast PEV sales from estimated trajectories of the corresponding explanatory factors for PEVs. Our approach for diurnal recharging load forecast is based on our conjecture that PEV users' recharging behaviors will demonstrate a gradual transition from a convenience driven mode to a cost driven mode in the next decade. The interactions between these two models are bidirectional: PEV sales forecast helps determine the recharging profile and consequently the recharging cost, which then feeds back to the multiple linear regression model as part of an explanatory factor. When the two models have reached an equilibrium after iterations of interactions, we obtain our final forecast for both PEV sales and the diurnal recharging load.

The sales and recharging load forecasting models are presented in Sections 3.2 and 3.3, respectively, and their interactions are explained in Section 3.4. We describe a case study in Section 3.5 and conclude the paper in Section 3.6.

3.2 PEV Sales Forecast Model

For the purpose of forecasting PEV sales, we use a multiple linear regression model, which attempts to describe the relationship between a response variable and a number of explanatory variables by fitting a linear equation to observed data. The following multiple linear regression model is used:

$$\log y_i^{\mathrm{P}} = \alpha_0^{\mathrm{P}} + \alpha_1^{\mathrm{P}} \log x_{i1}^{\mathrm{P}} + \alpha_2^{\mathrm{P}} \log x_{i2}^{\mathrm{P}} + ... + \alpha_k^{\mathrm{P}} \log x_{ik}^{\mathrm{P}} + \epsilon_i^{\mathrm{P}}, \quad \forall i = 1, ..., n. \tag{3.1}$$

Here y_i^{P} is the ith response variable, representing PEV sales in month i; $\{x_{i1}^{\mathrm{P}}, x_{i2}^{\mathrm{P}}, ..., x_{ik}^{\mathrm{P}}\}$ are k explanatory variables that are identified to be responsible for PEV sales; α_0^{P} is the intercept; $\{\alpha_1^{\mathrm{P}}, \alpha_2^{\mathrm{P}}, ..., \alpha_k^{\mathrm{P}}\}$ are the regression coefficients for the explanatory variables; ϵ_i^{P} is the ith error term; and the superscript 'P' is used to indicate 'PEV'. We take the logarithm function in the model to make the response variable more homoscedastic, and their coefficients can be interpreted as the sales elasticity:

$$\alpha_m^{\mathrm{P}} = \frac{\partial y_i^{\mathrm{P}} / y_i^{\mathrm{P}}}{\partial x_{im}^{\mathrm{P}} / x_{im}^{\mathrm{P}}}, \forall m = 1, 2, .., k.$$

An equivalent multiple linear regression model has been used in [2], in which yearly data are used to attribute electricity demand to several economic indicators.

Four explanatory variables have been identified for the regression model (3.1), which integrate a wide range of factors that may potentially influence PEV sales, including vehicle price, average mileage traveled, fuel efficiency, gasoline price, electricity price, tax incentives, recharging infrastructure availability, manufacturing capacity, etc. These explanatory variables emerged from a model selection procedure, which also included some other factors such as average personal income, national economic indicators, and media coverage of plug-in electric

vehicles. Our model selection procedure was based on data availability, correlations between factors, and significance of each factor on the response variable. The four explanatory variables that yield the best regression results are explained as follows.

- x_{i1}^{P} (in \$) is the average fuel cost savings in month i over a comparable ICEV. This variable can be computed using the following formula:

$$x_{i1}^{\mathrm{P}} = c_i^{\mathrm{I}} - c_i^{\mathrm{P}}. \tag{3.2}$$

  Here, c_i^{I} and c_i^{P} are the average fuel costs of ICEVs and PEVs in month i, respectively. Whereas the former depends on gasoline prices, miles traveled, and fuel efficiency, the latter also involves electricity prices, electric engine efficiency, and recharging behaviors. We will discuss the calculation of c_i^{I} later in Equation (3.4) and use c_i^{P} as an input parameter from Equation (3.8) of the recharging load forecasting model.

- x_{i2}^{P} (in \$) is the average tax credits for PEVs provided by the government in month i. This variable also represents the effect of various other government policies, which cannot all be reflected in a simple regression model.

- x_{i3}^{P} (in \$) is the average price difference between PEVs and their counterpart ICEVs in month i. We separate tax credits and the vehicle price premium as two variables because the former can only be received at the time of tax refund whereas the latter is paid upfront. Therefore, sales may respond differently to a \$1,000 tax rebate than a \$1,000 discount on the price tag [15].

- x_{i4}^{P} is the number of PEV models available in the market in month i. This variable takes into account the supply side constraints on PEV sales. Early adoption of Toyota Prius [13] and more recent situations with Chevrolet Volt [40] and Nissan Leaf [47] both show that the bottleneck of vehicle sales could be due to manufacturing capacity, materials supply, and/or other logistic constraints faced by vehicle manufacturers rather than consumer demand.

To forecast PEV sales, we need to obtain not only the forecast of these four explanatory variables but also an estimate of the regression coefficients that reflect the influences of explanatory variables on the PEV sales. Whereas the former can be obtained from existing studies [10], the latter is much more challenging due to the lack of observable data of PEV sales.

The approach we use to estimate the regression coefficients for PEV sales is to obtain an equivalent set of regression coefficients for HEV sales and use these for the PEV model (3.1). We use a similar multiple linear regression model for HEV sales:

$$\log y_i^{\mathrm{H}} \quad = \quad \alpha_0^{\mathrm{H}} + \alpha_1^{\mathrm{H}} \log x_{i1}^{\mathrm{H}} + \alpha_2^{\mathrm{H}} \log x_{i2}^{\mathrm{H}} + \alpha_3^{\mathrm{H}} \log x_{i3}^{\mathrm{H}} + \alpha_4^{\mathrm{H}} \log x_{i4}^{\mathrm{H}} + \epsilon_i^{\mathrm{H}}, \quad \forall i = 1, ..., n. \tag{3.3}$$

Here, y_i^{H} is the observed HEV sales in month i; ϵ_i^{H} is the ith error term; the four explanatory variables in (3.3) have similar meanings with their counterparts in (3.1) except that, as the superscript 'H' indicates, they are for 'HEV'. In particular, the explanatory variable x_{i1}^{H} is defined as the difference of weighted average fuel cost:

$$x_{i1}^{\mathrm{H}} = c_i^{\mathrm{I}} - c_i^{\mathrm{H}} = \sum_{j \in \mathcal{J}_i} w_{i,j}^{\mathrm{H}} g_i m_i \left(\frac{1}{f_j^{\mathrm{I}}} - \frac{1}{f_j^{\mathrm{H}}} \right), \tag{3.4}$$

where $\mathcal{J}_i$ is the set of ICEV models that are identified to be comparable with the HEV models available in the market in month i; $w_{i,j}^{\mathrm{H}}$ (in percentage) is the relative weight of the HEV model $j \in \mathcal{J}_i$ in month i; g_i (in \$/gallon) is the average gasoline price in month i; m_i (in miles) is the average miles traveled per vehicle in month i; f_j^{I} (in miles/gallon, or mpg) is the fuel efficiency of the ICEV that is comparable to HEV model j; and f_j^{H} (in mpg) is the fuel efficiency of the HEV model j. Since there exist more than 10 years of HEV sales data and all four explanatory variables can be computed using publicly available historical data, the regression coefficients for model (3.3) can be obtained relatively easily. We then use $\{\alpha_1^{\mathrm{H}}, \alpha_2^{\mathrm{H}}, \alpha_3^{\mathrm{H}}, \alpha_4^{\mathrm{H}}\}$ in model (3.1) as an estimate of $\{\alpha_1^{\mathrm{P}}, \alpha_2^{\mathrm{P}}, \alpha_3^{\mathrm{P}}, \alpha_4^{\mathrm{P}}\}$ for forecasting PEV sales.

This approach is based on an important assumption that the explanatory variables have similar effects on PEV sales as they have on HEV sales. Although this assumption ineluctably misses some factors that could drive PEV sales towards a different trajectory than HEVs had,

we argue that PEVs present consumers with the same tradeoff between fuel efficiency and price premium as HEVs do, only to a greater extent. Therefore it is reasonable to infer that consumer responses to these two types of fuel efficient vehicles would be comparable. After all, HEV sales are perhaps the most relevant and abundant data available for forecasting PEV sales.

3.3 PEV Recharging Load Forecast Model

Our approach to forecasting PEV recharging load is based on our conjecture that PEV users' recharging behaviors will show a gradual transition from a convenience driven mode in 2012 to a cost driven mode in 2020. Linear combinations of the two modes are used for the years in between, representing the gradual prevalence of smarter recharging infrastructures. In the convenience driven mode, the diurnal PEV recharging load curve is assumed to follow the same shape as the travel pattern curve that shows the average percentage of vehicles being parked at home. The rationale is that, since very limited recharging infrastructure is currently available beyond home garages, the more PEVs are parked at home at any given time, the more likely they are plugged in [14]. An example of the travel pattern from [24] is shown in Figure 3.1. The cost driven mode is assuming that the PEV recharging load will follow a "valley-filling" pattern of the baseline load curve. Figure 3.2 shows an example of valley-filling PEV recharging load. This assumption is motivated by two reasons. First, studies [19, 24, 23] have shown that uncontrolled PEV's recharging could have significant impacts on power systems. In view of the increasing interests and rapid development in smart-grid technologies, it appears reasonable to expect that some sort of control schemes will be put in place in order to coordinate PEV load and power system operation. Second, there is a strong positive correlation between the electricity load and the cost of electricity generation [46]. A "valley-filling" pattern is thus ideal for utilizing the idle capacity of power generators and minimizing recharging cost.

For a given travel pattern, $\beta_t, \forall t = 1, ..., 24$, that describes the average percentage of vehicles being parked at home, we can determine the convenience driven PEV recharging load (in MW)

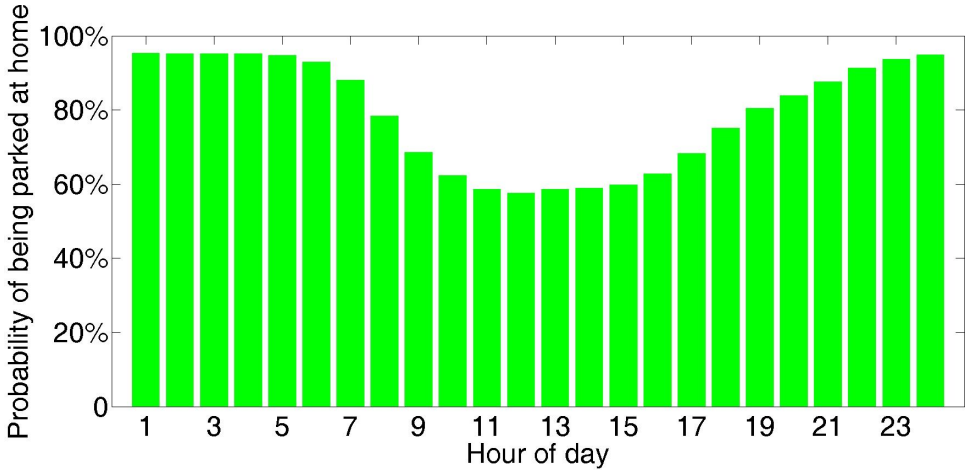

Figure 3.1 An example of travel pattern

as

$$\bar{r}_t = \frac{\beta_t}{\sum_{t=1}^{24} \beta_t} \rho N m^{\mathrm{E}}, \forall t = 1, ..., 24. \tag{3.5}$$

Here ρ (in MWh/mile) is the average PEV electricity efficiency factor; N is the number of PEVs on the road; and m^{E} (in miles) is the average distance traveled by the PEV fleet using electricity. Therefore, $\rho N m^{\mathrm{E}}$ is the daily electric energy consumption by the PEV fleet. We will use $\bar{r}_t(N, m^{\mathrm{E}})$ to denote the solution of (3.5) with N and m^{E} as input parameters.

For a given baseline load curve, $D_t, \forall t = 1, ..., 24$, we can determine the cost driven PEV recharging load by solving the following model:

$$\max_{r_t} \quad \min_t \{D_t + r_t\} \tag{3.6}$$

$$\text{s.t.} \quad \sum_t r_t = \rho N m^{\mathrm{E}}. \tag{3.7}$$

We will use $\hat{r}_t(N, m^{\mathrm{E}})$ to denote the solution to (3.6)-(3.7) with N and m^{E} as input parameters.

3.4 Interactions Between The Two Models

The sales and recharging load forecast models presented in Sections 3.2 and 3.3 are inter-dependent. On the one hand, both models (3.5) and (3.6)-(3.7) need the number of PEVs on the road as a parameter to determine the recharging behavior. Intuitively, if this number is

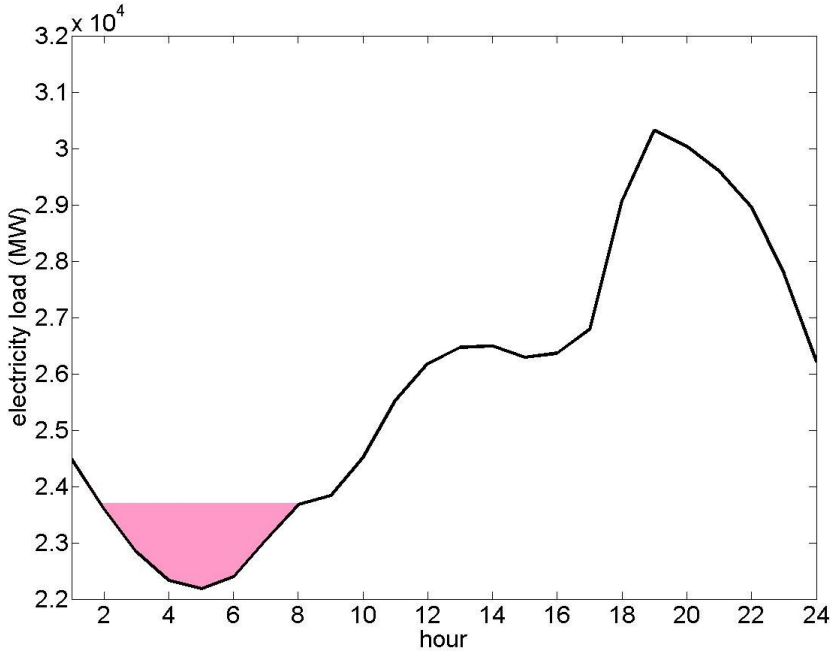

Figure 3.2 Valley-filling PEV recharging load

small, the recharging load would concentrate on the lowest valleys of the baseline load curve; otherwise, a larger number of PEVs would spread the recharging load to other hours of the day. On the other hand, the calculation of the explanatory factor x_{i1}^{P} in model (3.1) involves the average fuel cost of a PEV, c_i^{P}, which can be computed as follows:

$$c_i^{\mathrm{P}} = \sum_{t \in \mathcal{T}_i} \left\{ [(1-\theta_i)\bar{r}_t^{\top}(N_i, m_i^{\mathrm{E}}) + \theta_i \hat{r}_t^{\top}(N_i, m_i^{\mathrm{E}})]p_t + \frac{g_i m_i^{\mathrm{G}}}{24 f^{\mathrm{P}}} \right\}. \tag{3.8}$$

Since the PEV fleet includes both pure electric vehicles and plug-in hybrid electric vehicles, the fuel cost c_i^{P} includes cost of electricity and gasoline for distances driven by the electric and combustion engines, respectively. In (3.8), $\mathcal{T}_i$ is the set of hours in month i; N_i is the number of PEVs on the road in month i; $\bar{r}_t(N_i, m_i^{\mathrm{E}})$ and $\hat{r}_t(N_i, m_i^{\mathrm{E}})$ are the respective solutions from models (3.5) and (3.6)-(3.7), which are vectors of PEV recharging load of all nodes; θ_i is the combination parameter of the convenience driven and cost driven modes in month i; p_t (\$/MWh) is the vector of electricity prices for PEV load; m_i^{E} and m_i^{G} (in miles) are the daily average distance traveled by the PEV fleet using electricity and gasoline in month i, respectively; and f^{P} (in mpg) is the average fuel efficiency of the gasoline engine of PEVs.

Notice that N_i is the cumulative sales by month i:

$$N_i = \sum_{j=\max\{1,i-120\}}^{i} y_j^{\mathrm{P}}.$$

Here we are assuming that PEVs have a life time of 10 years (or 120 months) [29], thus the lower limit of the summation.

We compute the prices of recharging load p_t using locational marginal prices (LMPs). Since the deregulation of electricity markets in the 1990s, LMPs have been adopted by six (CAISO, MISO, ISO-NE, NYISO, PJM, and ERCOT) out of ten national electricity markets in the U.S. The LMPs are calculated as the incremental cost of re-dispatching the power system to serve one more unit of demand in a given time and location subject to generation and transmission constraints. LMPs differ by time and by location [46]. Temporal differences are largely caused by realtime demand fluctuation, and spatial differences are due to the lack of transmission lines to deliver the least expensive power to all demand zones. Whereas LMPs are influenced by various factors such as load uncertainty, thermal limit, capacity reserve and market power, we estimate LMPs solely based on electricity loads. This is because electricity load is the most influential factor that drives the LMP curves [46], evidenced by their strong correlation observed in historical data. Moreover, electricity load forecast data are much more readily available than other electricity market data. Assuming we have a data set of historical electricity load and associated LMPs $\{D_\tau^{\mathrm{h}}, p_\tau^{\mathrm{h}}\}, \forall \tau \in \mathcal{H}$, a forecast of baseline electricity load D_t, and a given PEV load r_t, we use the following k-nearest neighbors algorithm [26] to compute the LMP p_t:

Step 1: Obtain $\mathcal{T}$, a set of $K = 20$ hours $\mathcal{T} \subset \mathcal{H}$ that have the smallest differences between D_τ^{h} and $D_t + r_t$:

$$||D_\tau^{\mathrm{h}} - (D_t + r_t)||_2 \leq ||D_{\tau'}^{\mathrm{h}} - (D_t + r_t)||_2, \forall \tau \in \mathcal{T}, \tau' \in \mathcal{H} \backslash \mathcal{T}.$$

Step 2: Compute the LMP p_t as $p_t = (1+\lambda)^t \sum_{\tau \in \mathcal{T}} p_\tau^{\mathrm{h}} / K$, where λ represents an estimated LMP growth rate.

3.5 Case Study

A case study is conducted in the Midwest Independent Transmission System Operator (MISO) area, which is an independent system operator that provides transmission service to all or parts of 13 U.S. states in the midwest area and the Canadian province of Manitoba [30]. We only consider the states in the U.S. and divide these into east, central, and west regions, as shown in Figure 3.3. It is estimated that PEV sales in the east, central, and west regions of MISO account for, respectively, 6.5%, 6.6%, and 6.7% of total sales in the U.S., based on the numbers of passenger cars as percentages of all the registered vehicles in the U.S. [2].

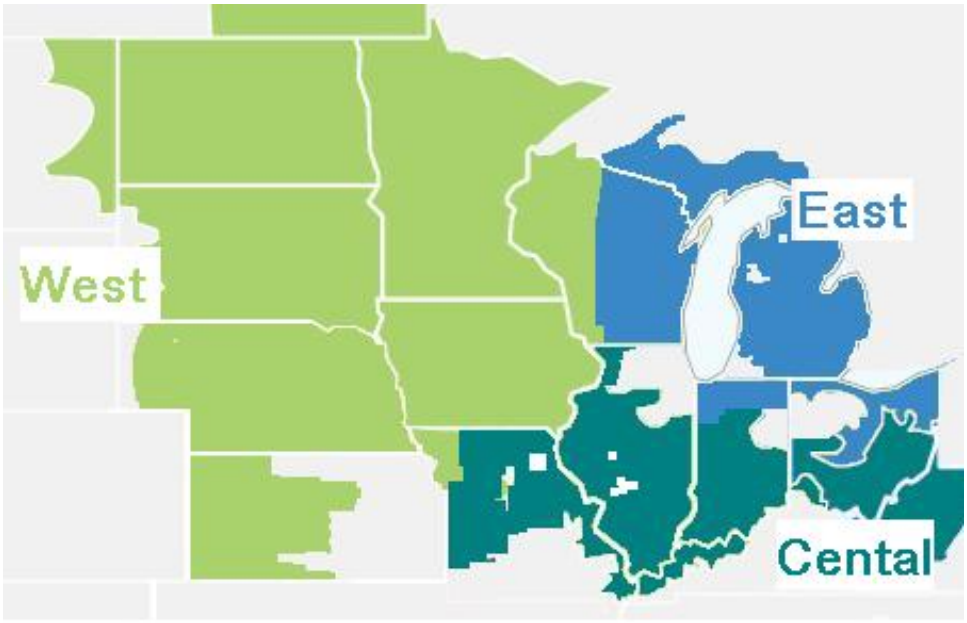

Figure 3.3 MISO area.

We obtained forecasting results for three scenarios: reference, low, and high. We use publicly available forecast data for the reference scenario, and make them less (more) favorable for PEV sales for the low (high) scenario.

3.5.1 Data Sources

The data and data sources used for our case study are summarized as follows.

- x_{i1}^{H}: Evaluated using Equation (3.4) with the following parameters.
  - $\mathcal{J}_i$: We found 23 HEV models in the U.S. market between 1999 and 2009. They are listed in Table 3.1 along with their comparable ICEVs. Figure 3.4 also provides information about the available HEV models in any month i.

Table 3.1 Comparable ICEVs to HEVs

	HEV	Comparable ICEV
1	Honda Insight Hybrid	Honda Civic Sedan
2	Toyota Prius	Toyota Corolla Sedan
3	Honda Civic Hybrid	Honda Civic Sedan
4	Ford Escape Hybrid	Ford Escape
5	Honda Accord Hybrid	Honda Accord Sedan
6	Mercury Mariner Hybrid	Mercury Mariner
7	Toyota Highlander Hybrid	Toyota Highlander V6
8	Lexus RX 400h	Lexus RX 330
9	Toyota Camry Hybrid	Toyota Camry Sedan LE
10	Lexus GS 450h	Lexus GS 350
11	Nissan Altima Hybrid	Nissan Altima
12	Saturn Vue Hybrid	Saturn Vue
13	Lexus LS 600hL	Lexus LS 460L
14	Saturn Aura Hybrid	Saturn Aura
15	Chevy Malibu Hybrid	Chevy Malibu
16	Cadilac Escalade	Cadilac Escalade
17	GMC Yukon 1500 Hybrid	GMC Yukon 1500
18	Chevy Tahoe Hybrid	Chevy Tahoe 1500
19	Chrysler Aspen Hybrid	Chrysler Aspen
20	Lexus HS 250h	Lexus IS 250
21	Dodge Durango Hybrid	Dodge Durango
22	Ford Fusion Hybrid	Ford Fusion
23	Mercury Milan Hybrid	Mercury Milan

  - $w_{i,j}^{\mathrm{H}}$: Figure 3.4 shows the yearly market share [33] of the manufacturer of HEV model j from 1999 to 2009. We hold $w_{i,j}^{\mathrm{H}}$ constant for all 12 months of the year in our calculation, although they are plotted continuously to better illustrate the dynamics.
  - g_i, m_i, f_j^{I}, f_j^{H}: Historical and forecast data are from [44] and [41].
- x_{i2}^{H}, x_{i3}^{H}, x_{i4}^{H}, y_i^{H}: Data are from [42], [6], and [17].

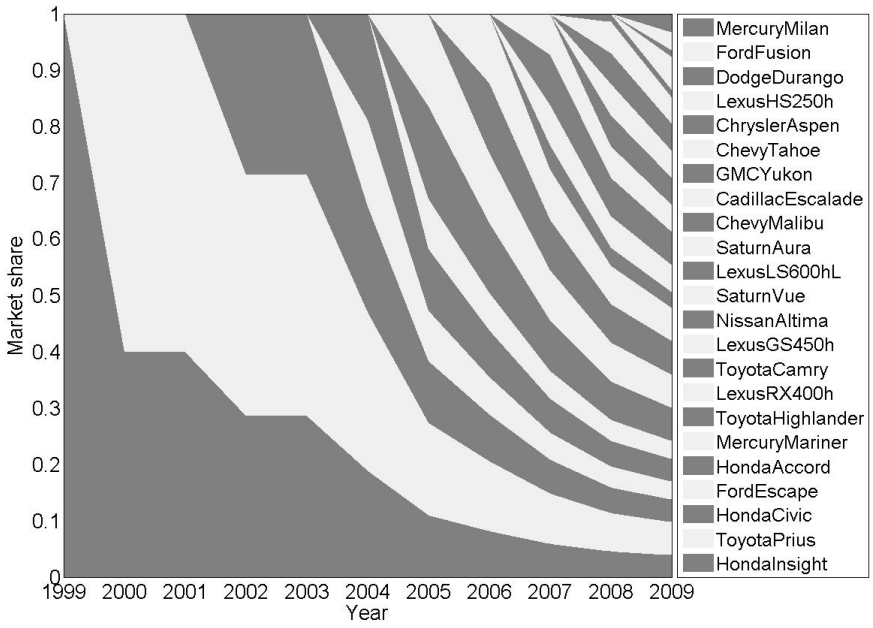

Figure 3.4 Market shares of HEVs from 1999 to 2009

- c_i^{I}, x_{i2}^{P}, x_{i3}^{P}, x_{i4}^{P}: Data for the three cases are summarized in Tables 3.2-3.4, some of which are from [2, 10, 1] and others assumed.

- m^{E}, m^{G}: Total miles driven ($m^{\mathrm{E}} + m^{\mathrm{G}}$) data are from [2]. We assume that 80% of these miles are powered by electricity and 20% by gasoline in 2012, and this ratio is linearly increased to 95% vs. 5% in 2020. This assumption is based on a related study by [5], who introduced the term "utility factor", meaning the percentage of miles driven by electric vehicles in electric mode. The utility factors for Chevrolet Volt and Nissan Leaf are 0.64 and 1.0, respectively [28]. Our assumption is equivalent to a 0.8 utility factor for the whole PEV fleet in 2012, which increases to 0.95 due to expected future development of PEV battery technology and recharging infrastructure that will substitute more gasoline miles with cheaper electricity miles.

- f^{P}: Data are from [44].

- α_0^{P}: Intercept is equal to 18.6, which is calculated from the sales data [16, 22, 34, 27] of Chevrolet Volt (5,329) and Nissan Leaf (8,066) between December 2010 and October

2011 in the U.S.

- D_t: Historical actual load data between April 2005 and June 2010 are from [30]. Future baseline load data are predicted based on historical data with 0.7% annual increase according to [44].
- ρ: Assumed to be equal to the electricity efficiency of Chevrolet Volt, which is 36 kWh per 100 miles [41].
- D_τ^{h}, p_τ^{h}: Hourly data between April 2005 and June 2010 are from [30].
- β_t: Data are from [24].
- θ_i: According to [21], "[t]he implementation of smart meters can be assumed to follow the shape of a logistic curve with exponential growth initially, followed by a slowing growth and finally reaching maturity as most households are equipped with smart meters." Assuming a growth rate between 0.7 and 0.8, we estimate θ_i to be 1.6%, 4.2%, 8.8%, 15.5%, 24.3%, 35.1%, 48.0%, 63.0%, 80% from 2012 to 2020, respectively. All months within a year are assumed to be the same.
- λ: LMP growth rate is set to be -0.2%, which is from [44].

3.5.2 Results

3.5.2.1 HEV Sales Regression Model

Coefficients of the HEV sales regression model are summarized in Table 3.5. As expected, α_1^{H} (fuel savings), α_2^{H} (tax credits), and α_4^{H} (number of vehicle models) all have positive influences on the sales, whereas α_3^{H} (price premium) has a negative influence. As suggested by the values of α_2^{H} and α_3^{H}, instant savings have a much higher impact on sales than tax credits that only apply to next year's income tax filing. This observation is consistent with the findings from [15].

The R^2 value of the model is 80.31%, which means that a large proportion of variability in the historical sales can be explained by the four explanatory variables that we identified; it also

suggests trustworthy predictions for future sales. In contrast, the naive random walk model's R^2 value is 61.21%. The p-values in Table 3.5 for all explanatory variables are small enough to justify their significance. The VIFs (Variance Inflation Factors) are also smaller than 5 for all explanatory variables, indicating little multicollinearity between them. Figure 3.5 compares the residual plots with and without taking logarithm in model (3.1); it shows that the variance of the response variable has been stabilized by the logarithm function. Table 3.6 shows the correlations between response and explanatory variables, suggesting strong linear relationships. We use the historical HEV sales for year 2010 and 2011 as the hold out sample to verify our model. The mean absolute percentage errors of monthly sales forecast for year 2010 and 2011 are 14.62% and 22.70%, respectively. The predicted HEV annual sales for year 2010 and 2011 are 272,919 and 266,194, compared to actual sales of 274,210 and 268,752, respectively [23].

3.5.2.2 PEV Sales Forecast

We compare our PEV sales results with those from the literature. As shown in Figure 3.6, our forecast results of the cumulative PEV sales curves in the U.S. in the low and high cases form a triangle shaped area. The reference case curve is plotted inside the area. Compared to Obama's expectation of 1 million PEVs by 2015, our forecasts are much less optimistic with 2017 and 2020 as the respective years to pass the 1 million mark in the high and reference cases, and even later in the lower case. The Morgan Stanley forecast is close to our low case until 2016, and then gradually increases to the same level as our reference case in 2020. The ORNL study forecasts that Obama's goal can be achieved in the high case, but even its low case exceeds our high case forecast beyond 2016. The PNNL study forecasts a sharp PEV proliferation, with its low case close to our low case until 2015 and then sharply increases to exceed ORNL's high case in 2020. EPRI's forecast is the most optimistic one, with its low case only slightly lower than PNNL's high case. In comparison, the medium case sales forecasts for 2020 are 1 million, 1 million, 2.8 million, 3.4 million, and 15 million by this paper, Morgan Stanley, ORNL, PNNL, and EPRI, respectively.

Notice that the original forecast results of PNNL and EPRI are given in penetration rates (percentage of new vehicle sales) rather than in actual number of PEV sales. The results shown in Figure 3.6 are obtained by multiplying their penetration rates by the number of new vehicle sales forecast from [10]. We also point out that our study is conducted a few years later than Morgan Stanley [4], PNNL [6], EPRI [3], and ORNL [19], thus having the advantageous access to more information and data.

3.5.2.3 Diurnal PEV Recharging Load Curve

We plot our forecast results of the diurnal PEV recharging load profiles in the low case in Figure 3.7, which are normalized diurnal load curves that represent the percentages of the daily energy consumption. As such, the areas below all profiles are equal to 1.0. The results demonstrate a clear transition of recharging behaviors in the next decade. In 2012, the recharging load spreads to all 24 hours of the day with slightly higher consumption in the nighttime when more vehicles are parked at home. Towards 2020, a unimodal in the early morning between 2 AM and 6 AM starts to emerge and becomes the concentration of recharging load, which consequently reduces the recharging profile in other hours of the day.

Figure 3.8 demonstrates a similar pattern for the high case, but the recharging load profiles are less concentrated to the unimodal than in the low case. This is because in the high case, a larger percentage of recharging load spills out of the valley of the baseline load to other hours of the day.

The impact of PEV recharging load on the total electricity load curve in 2020 is shown in Figure 3.9. The early morning valley of the baseline load curve is slightly filled by the PEV recharging load, which indicates a modest and manageable impact of PEV recharging load on power systems. For the first few years of the 2010s, this impact is expected to be negligible. Our results suggest that, PEVs are not likely to place an overwhelming burden to power systems in the next decade, as long as the development of smarter recharging infrastructures can catch up with the growth of PEV sales.

3.6 Conclusions and Discussions

In this paper, we have presented two interactive models to jointly forecast PEV sales and the diurnal recharging load curve. Compared to existing approaches, our study makes the following new contributions. First, multiple factors are explicitly incorporated in the multiple linear regression model for PEV sales forecast, including gas prices, electric rates, fuel efficiency, miles driven, vehicle prices, tax credits, and supply side constraints. Second, we study decade-long historical data of HEV sales and other factors to extract information about how consumers make the tradeoff among upfront vehicle price, long-term fuel cost, and other factors when purchasing new vehicles, which is utilized in the PEV sales forecast model. Third, we propose the convenience driven and cost driven modes to describe the transition of PEV users' recharging behaviors as a result of gradually prevailing smarter recharging infrastructures. Fourth, our approach explicitly incorporates the interdependencies between sales forecast and recharging load forecast models. Last but not least, our models can be used to answer "what if" questions. For example, what would happen to PEV sales if gas prices increase to \$20/gallon in 2020, or if real-time electric rates and fast recharging meters are made widely available by 2015, or if rare earth supplies limit the number of PEV manufacturers?

Our approach is also inevitably not without caveats. The PEV sales forecasting model, for example, does not explicitly consider the competition from HEVs in the market, which could potentially result in overestimation of PEV sales. However, we argue that the lines have become so increasingly blurred between HEVs and ICEVs in terms of fuel efficiency that HEVs can be considered as a small subset (2% in new vehicle sales in the U.S. in the first ten months of 2011 [23]) of ICEVs. In fact, several ICEVs (Toyota Corolla, 30 mpg; Honda Civic, 29 mpg) are no less fuel efficient than some HEVs (Lexus GS 450h, 24 mpg; Saturn Aura, 30 mpg). Another limitation of our model is that the lagging effect is not explicitly taken into consideration. Moreover, our models cannot accommodate other unforeseeable factors that could change the dynamics of the vehicle market, such as rapid development of other vehicle technologies (fuel cell, hydrogen, solar), high speed rail, or public transportation.

Future research directions include surveying of early PEV users when sufficient samples are accessible, designing electric rates and recharging facilities to effectively control recharging loads, and investigating the viability of harnessing intermittent renewable energy to recharge PEVs.

Table 3.2 Data for the reference case

year	c_i^{I} (\$)	x_{i2}^{P} (\$)	x_{i3}^{P} (\$)	x_{i4}^{P} (count)
2012	204.1	7,500	7,200	10
2013	211.7	7,500	7,000	14
2014	217.0	6,500	6,900	18
2015	218.6	5,500	6,900	22
2016	221.3	4,500	6,800	26
2017	223.7	3,500	6,700	30
2018	228.8	2,500	6,600	34
2019	235.5	1,500	6,600	38
2020	242.5	500	6,500	42

Table 3.3 Data for the high case

year	c_i^{I} (\$)	x_{i2}^{P} (\$)	x_{i3}^{P} (\$)	x_{i4}^{P} (count)
2012	209.6	7,500	7,100	14
2013	219.8	7,500	6,900	20
2014	228.5	7,500	6,700	26
2015	237.2	7,500	6,600	32
2016	245.9	7,500	6,700	38
2017	250.9	7,500	6,300	44
2018	255.0	7,500	6,000	50
2019	264.2	7,500	5,900	55
2020	276.5	7,500	5,800	59

Table 3.4 Data for the low case

year	c_i^{I} (\$)	x_{i2}^{P} (\$)	x_{i3}^{P} (\$)	x_{i4}^{P} (count)
2012	194.2	7,500	7,100	7
2013	196.2	7,500	7,200	10
2014	197.3	5,500	7,300	13
2015	197.3	3,500	7,300	16
2016	193.6	1,500	7,200	18
2017	193.5	500	7,300	20
2018	193.0	500	7,400	22
2019	193.4	500	7,500	23
2020	193.7	500	7,500	24

Table 3.5 HEV sales regression coefficients

coefficient	estimate	std error	t ratio	p-value	VIF
α_0^{H}	21.16	4.44	4.76	<0.0001*	.
α_1^{H}	0.87	0.12	7.29	<0.0001*	1.02
α_2^{H}	0.12	0.04	2.69	0.0090*	3.35
α_3^{H}	–1.86	0.51	–3.61	0.0006*	2.11
α_4^{H}	0.38	0.12	3.15	0.0024*	4.80

Table 3.6 Correlations between response variable and each explanatory variable

	$\log\, y^{\mathrm{H}}$	$\log x_1^{\mathrm{H}}$	$\log x_2^{\mathrm{H}}$	$\log x_3^{\mathrm{H}}$	$\log x_4^{\mathrm{H}}$
$\log\, y^{\mathrm{H}}$	1.00	0.33	0.69	–0.68	0.78

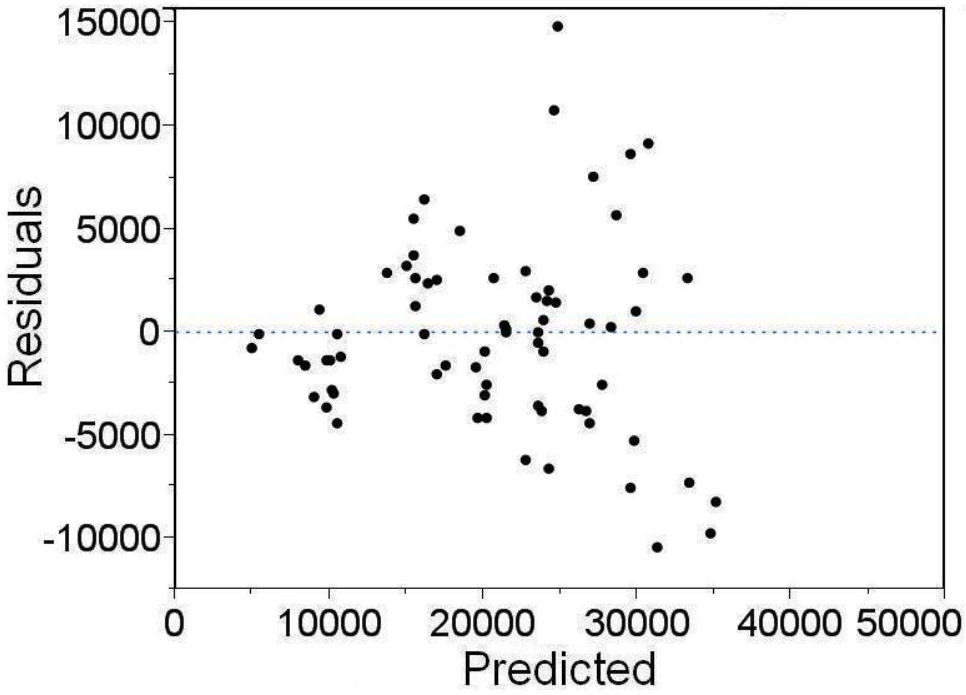

(a) Regular scale

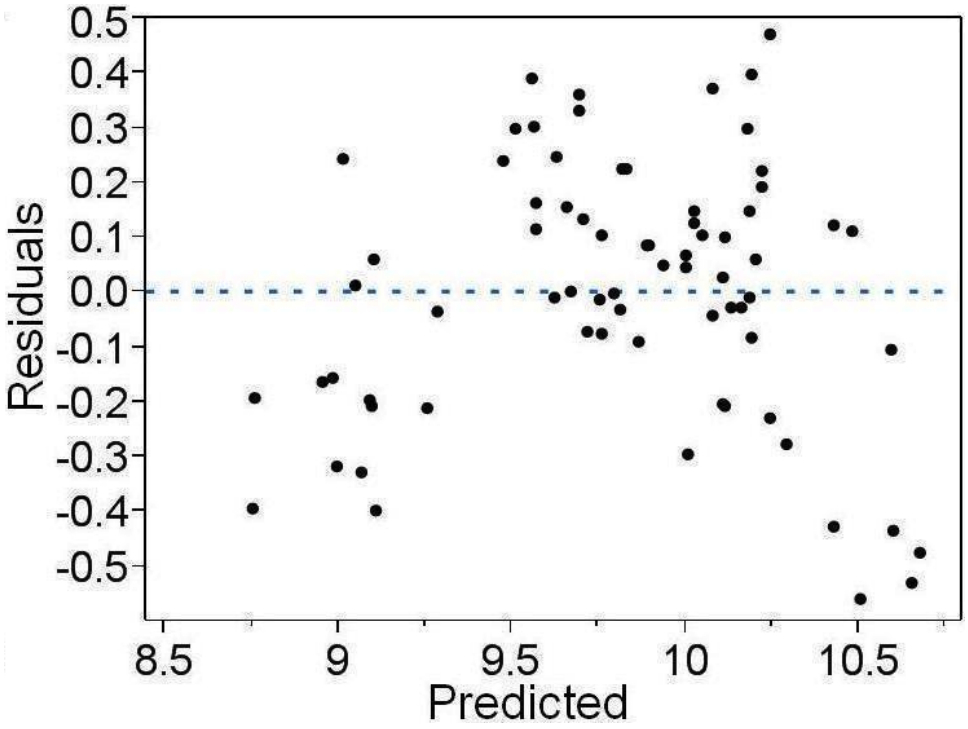

(b) Logarithm scale

Figure 3.5 Residual plots

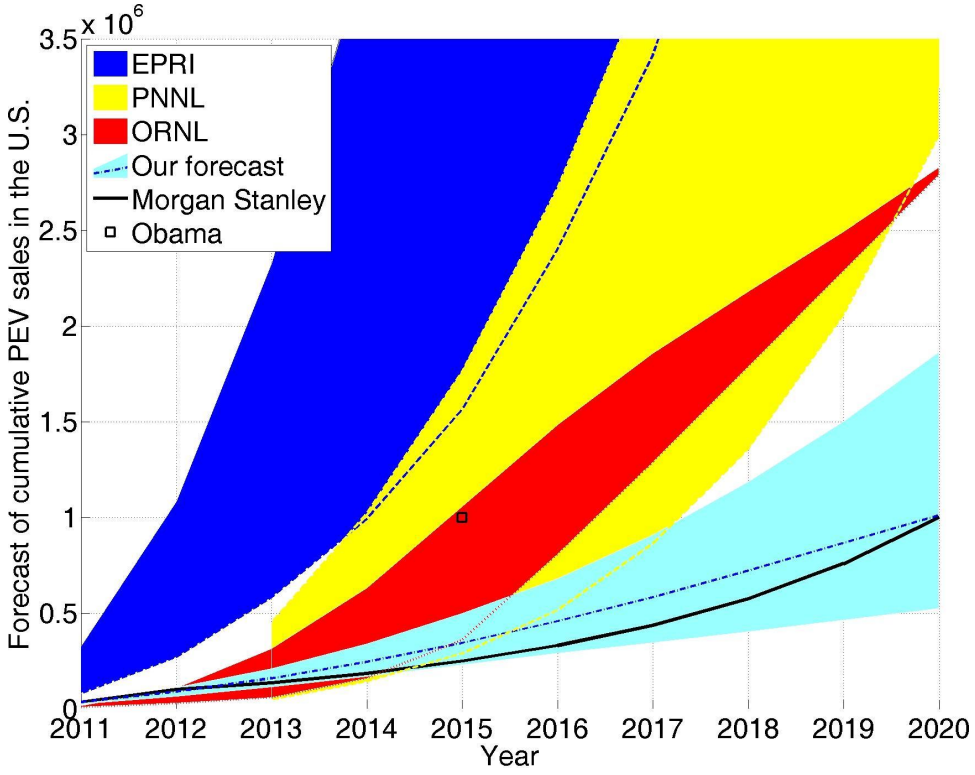

Figure 3.6 PEV cumulative sales forecast in the U.S.

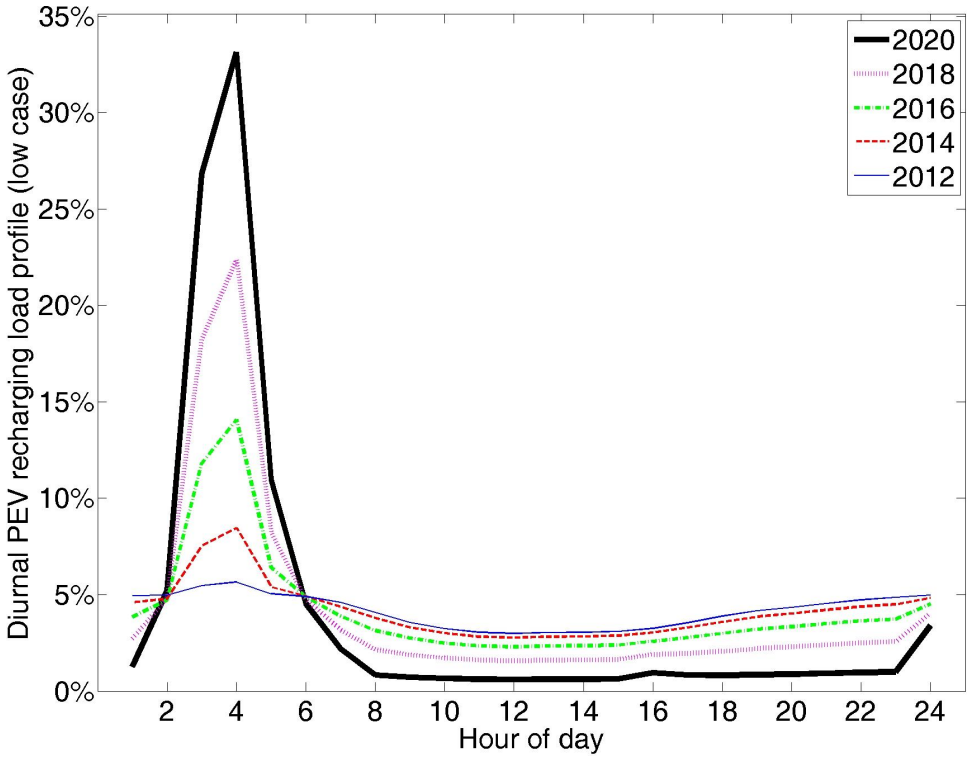

Figure 3.7 Diurnal PEV recharging load profile (low case)

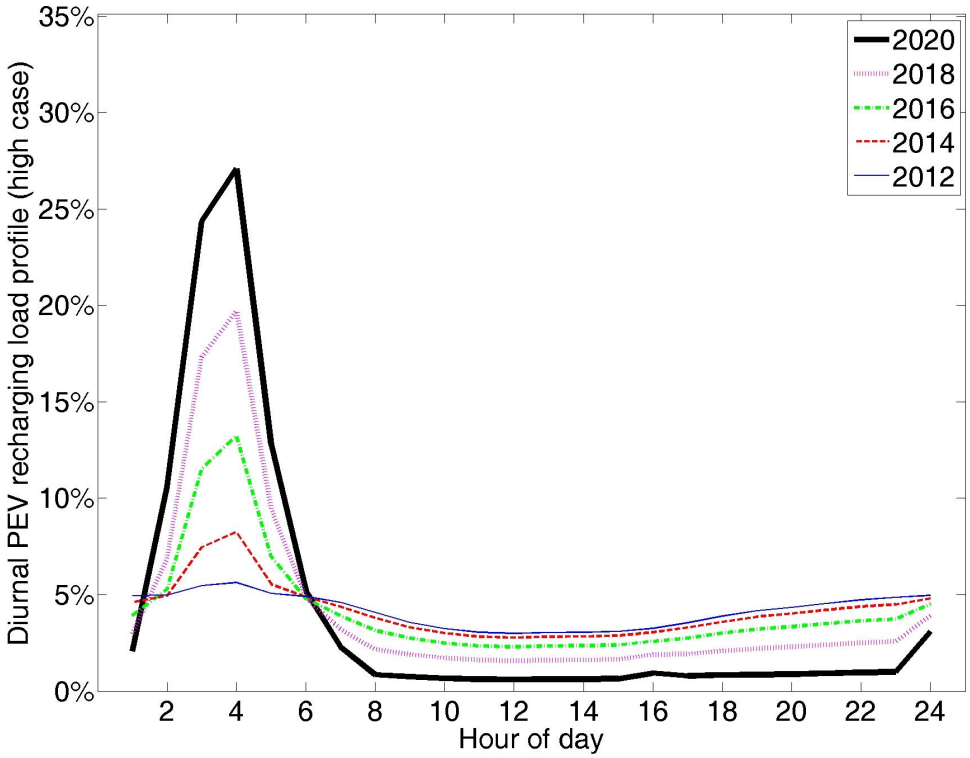

Figure 3.8 Diurnal PEV recharging load profile (high case)

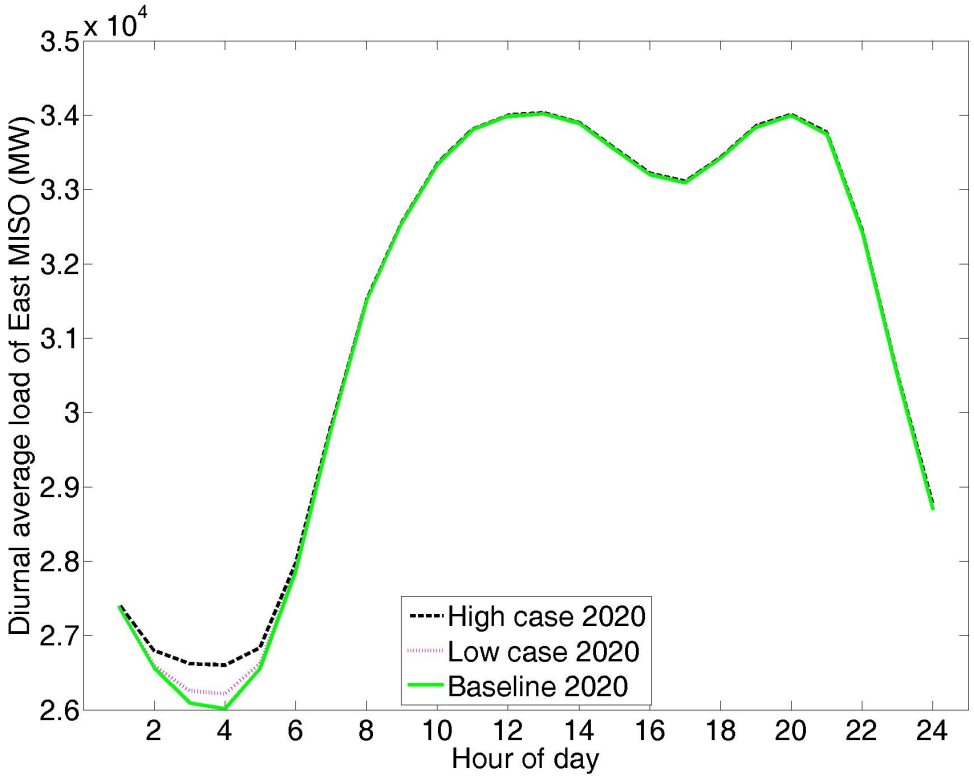

Figure 3.9 Baseline and PEV recharging load

Bibliography

[1] "Transitions to alternative transportation technologies – plug-in hybrid electric vehicles," USA: National Academies Press, Washington, DC, 2010.

[2] I. Azevedo, M. Morgan, and L. Lave, "Residential and regional electricity consumption in the US and EU: How much will higher prices reduce CO2 emissions?" *The Electricity Journal*, 2011.

[3] P. Balducci, "Plug-in hybrid electric vehicle market penetration scenarios," Tech. Rep., Department of Energy, 2008.

[4] A. Bandivadekar, K. Bodek, L. Cheah, C. Evans, T. Groode, J. Heywood and M. Weiss. "On the Road in 2035: Reducing transportations petroleum consumption and GHG emissions, laboratory for energy and the environment," Tech. Rep., Massachusetts Institute of Technology, 2008.

[5] T. Bradley and C. Quinn. "Analysis of plug-in hybrid electric vehicle utility factors," *Journal of Power Sources*, vol. 195, no. 16, pp. 5399-5408, 2010.

[6] www.cars.com.

[7] K. Clement-Nyns, E. Haesen, and J. Driesen, "The impact of charging plug-in hybrid electric vehicles on a residential distribution grid," *IEEE Transactions on Power Systems*, vol. 25, no. 1, pp. 371–380, 2010.

[8] P. Davidson, "Buzz grows for modernizing energy grid," *USA TODAY*, January 29, 2009.

[9] P. Denholm and W. Short, "An evaluation of utility system impacts and benefits of optimally dispatched plug-in hybrid electric vehicles," Tech. Rep., National Renewable Energy Laboratory, 2006.

[10] DOE/EIA-0383, "Annual energy outlook 2011 with projections to 2035," *Energy Information Administration: Washington, DC*, 2011.

[11] M. Duvall and E. Knipping, "Environmental assessment of plug-in hybrid electric vehicles. volume 1: Nationwide greenhouse gas emissions," Tech. Rep., EPRI, Palo Alto, CA. 1015325, 2007.

[12] A. Elgowainy, Y. Zhou, A. Vyas, M. Mahalik, D. Santini, and M. Wang. "Impacts of charging choices for plug-in hybrid electric vehicles in 2030 scenario," *Transportation Research Record: Journal of the Transportation Research Board*, vol. 2287, no. 1, pp. 9-17, 2012.

[13] S. Freeman, "Forget rebates: The hybrid-car markup," *Wall Street Journal*, 2004.

[14] www.fueleconomy.gov.

[15] K. Gallagher and E. Muehlegger, "Giving green to get green? Incentives and consumer adoption of hybrid vehicle technology," *Journal of Environmental Economics and Management*, vol. 61, no. 1, pp. 1–15, 2011.

[16] General Motors. www.gm.com.

[17] Green Car Congress. www.greencarcongress.com.

[18] S. Hadley, "Impact of plug-in hybrid vehicles on the electric grid," Tech. Rep., Oak Ridge National Laboratory, 2006.

[19] S. Hadley, and A. Tsvetkova. "Potential impacts of plug-in hybrid electric vehicles on regional power generation," Tech. Rep., Oak Ridge National Laboratory, ORNL/TM-2007/150, 2008.

[20] S. Hadley and A. Tsvetkova, "Potential impacts of plug-in hybrid electric vehicles on regional power generation," *The Electricity Journal*, vol. 22, no. 10, pp. 56–68, 2009.

[21] S. Heinen, et al. "Impact of Smart Grid Technologies on Peak Load to 2050," 2011.

[22] J. Holmes, "GM September 2011 sales climb 20 percent on back of Chevrolet Cruze, truck sales," *Motor Trend*, 2011.

[23] www.hybridcars.com.

[24] M. Kintner-Meyer, K. Schneider, and R. Pratt, "Impacts assessment of plug-in hybrid vehicles on electric utilities and regional U.S. power grids part 1: Technical analysis," Tech. Rep., Pacific Northwest National Laboratory, 2007.

[25] J. Kliesch and T. Langer, "Plug-in hybrids: An environmental and economic performance outlook," Tech. Rep., American Council for an Energy-Efficient Economy, 2006.

[26] A. Lora, J. Santos, A. Expósito, J. Ramos, and J. Santos, "Electricity market price forecasting based on weighted nearest neighbors techniques," *IEEE Transactions on Power Systems*, vol. 22, no. 3, pp. 1294–1301, 2007.

[27] E. Loveday, "Chevy Volt outsells Nissan Leaf in October," *PluginCars*, 2011.

[28] Lutsey, Nicholas, and D. Sperling. "Regulatory adaptation: Accommodating electric vehicles in a petroleum world." *Energy Policy*, vol. 45, pp. 308-316, 2012.

[29] V. Marano, S. Onori, Y. Guezennec, G. Rizzoni, and N. Madella. "Lithium-ion batteries life estimation for plug-in hybrid electric vehicles," Vehicle Power and Propulsion Conference, IEEE, pp. 536-543, 2009.

[30] Midwest ISO. www.misoenergy.org.

[31] M. Stanley, "Plug-in hybrids: The next automotive revolution," Tech. Rep., Morgan Stanley, 2008.

[32] K. Morrow, D. Karner, and J. Francfort. "Plug-in hybrid electric vehicle charging infrastructure review," US Department of Energy-Vehicle Technologies Program, 2008.

[33] Motor Intelligence. www.motorintelligence.com.

[34] X. Nissan, "Nissan North America sales rise 25.3% in September," *PRNewswire*, 2011.

[35] K. Parks, P. Denholm, and T. Markel, "Costs and emissions associated with plug-in hybrid electric vehicle charging in the Xcel energy Colorado service territory," Tech. Rep., National Renewable Energy Laboratory, 2007.

[36] S. Plotkin and M. Singh. "Multi-path transportation futures study: vehicle characterization and scenario analyses," Tech. Rep., Argonne National Laboratory (ANL), 2009.

[37] M. Scott, M. Kintner-Meyer, D. Elliott, and W. Warwick, "Impacts assessment of plug-in hybrid vehicles on electric utilities and regional U.S. power grids part 2: Economic assessment," Tech. Rep., Pacific Northwest National Laboratory, 2007.

[38] K. Sikes, T. Gross, Z. Lin, J. Sullivan, T. Cleary, and J. Ward, "Plug-in hybrid electric vehicle market introduction study: Final report," Tech. Rep., 2010, Oak Ridge National Laboratory (ORNL).

[39] A. Simpson, "Cost-benefit analysis of plug-in hybrid electric vehicle technology," Tech. Rep., National Renewable Energy Laboratory, 2006.

[40] "Limited supplies keep sales of Chevy Volt, Nissan Leaf down," *Gazette*, 2011.

[41] United States Environmental Protection Agency. www.epa.gov.

[42] U.S. Department of Energy. www.energy.gov.

[43] U.S. Department of Transportation. www.dot.gov.

[44] U.S. Energy Information Administration. www.eia.gov.

[45] L. Wang, A. Lin, and Y. Chen, "Potential impacts of plug-in hybrid electric vehicles on locational marginal prices and emissions," *Naval Research Logistics*, vol. 57, no. 8, pp. 686–700, 2010.

[46] L. Wang and M. Mazumdar, "Using a system model to decompose the effects of influential factors on locational marginal prices," *IEEE Transactions on Power Systems*, vol. 22, no. 4, pp. 1456–1465, 2007.

[47] J. Welsh, "Short Leaf supply could cost Nissan sales," *Wall Street Journal*, 2011.

[48] D. Wu, D. Aliprantis, and K. Gkritza, "Electric energy and power consumption by light-duty plug-in electric vehicles," *IEEE Transactions on Power Systems*, vol. 26, no. 2, pp. 738–746, 2011.

CHAPTER 4. MEASURING AND MITIGATING PLUG-IN ELECTRIC VEHICLES' POTENTIAL IMPACT ON POWER SYSTEMS

Zhaoyang Duan and Lizhi Wang

4.1 Introduction

With its ascending sales and ability to recharge batteries from external electric power outlet, plug-in electric vehicle (PEV) poses a series of both new advantages and challenges to the power systems [6, 19, 4, 9]. Although many studies have been conducted to assess PEVs' influence from various aspects, few of them view their potential impact from recharging uncertainty perspective and study how to effectively mitigate the uncertainty by optimizing electricity rates. The importance of these two topics are based on the following facts. Firstly, besides the increasing number of PEV fleet, whether the additional recharging load is added onto peak or off-peak load hours of baseline load indeed makes difference on the generation burden for the power systems. Moreover, the flexibility of PEV users' recharging behavior is the main reason that causes the uncertainty of PEVs impact to the power systems. Secondly, to adjust PEV users recharging behavior and further control their impact on the power systems, electricity rates and PEV users response program are important and effective tools to utilize. Therefore, in this paper, we define two measurements to assess PEVs' impact from both magnitude and uncertainty perspectives, study how PEV users recharging behavior responses to the electricity rates, and optimize the electricity rates that can effectively mitigate PEVs uncertainty of impact to the power systems.

Previous studies show that PEVs impact on the power systems are from various of perspectives. For example, Denholm and Short [8] evaluate the impacts and benefits of optimally

dispatching PHEVs on power systems. Wang et al. [23] analyze the impact of PHEVs on locational marginal prices. S. Hadley [10] uses ORCED model to evaluate the impact of PHEVs on Virginia-Carolinas electric grid in 2018. The results include the impacts on capacity requirements, fuel types, generation technologies, and emissions. C. Roe et al. [16] investigate the impacts of PHEVs on power systems infrastructure and primary fuel utilizations. K. Clement-Nyns et al. [7] study the PHEVs' impact on the distribution grid in terms of power losses and voltage deviations. K. Schneider et al. [17] present the results of PEVs' impact specifically for pacific northwest distribution systems. G. Putrus et al. [15] focus on the impact of PEVs on the future design of power networks and potential violations of voltage limits. Different from these literatures, our paper establishes two quantitative risk measures to evaluate PEVs impact to the power systems. Besides the increasing magnitude of recharging load, the uncertainties of PEV users recharging time, location, and amount of load also generate significant impact. Thus, the two risk measures not only consider the direct incremental cost, but also economic uncertainties that PEVs could pose to the power systems.

To mitigate PEVs impact, smart grid is a mostly utilized network which can intelligently integrate information of electric suppliers and consumers and provide efficient services. There exists two ways for power utilities to control PEVs recharging impact. In the first way, smart grid network utilizes a centralized PEV aggregator to manage the recharging time for every PEV. The aggregator limits the number of PEVs that are actually recharging according to the status of the total generation capacity. This approach could effectively control the amount of recharging load for peak hours, but largely reduce the convenience for consumers. For PEV users, plugging in their vehicles doesn't necessarily mean it's recharging unless the aggregator allows to. In the second way, smart grid utilizes time-of-use (TOU) electricity rate and demand response program to effectively adjust PEV users recharging behavior. TOU rate gives PEV users price incentives to voluntarily adjust their normal energy consumption pattern to an economically optimal way, and a price-based demand response program is capable of managing load balance on the demand side. In this more applicable approach, PEV users are able to make decision of their recharging time based on given electricity rates. Numerous studies have been

conducted on the implementation of TOU rate and demand response program. Walawalkar et al. [22] provide an overview of the evolution of the demand response programs in PJM and NY-ISO markets. Horowitz et al. [12] explore three voluntary service options, including real-time pricing, TOU pricing, and interruptible service, in order to encourage residential customers to alter their electricity usage in response to the changes of electricity price. Dynamic pricing is implemented to reduce peak load demand in Australia [20]. Shao et al. [18] analyze the impact of TOU rates on customer behaviors in a residential community. Their results show that TOU rate can be properly designed to reduce the peak demand even with the presence of PEVs. In this paper, our study is based on the second controlling approach. We also assume that separating from baseline load, PEV load utilize special electricity rates system and recharging infrastructure so that PEVs face different electricity rates from normal electric assumptions.

This paper focuses on assessing the potential impact of PEVs recharging load on power systems, and optimizing the electricity rates that can effectively mitigate the impact of PEVs recharging load with incorporation of PEV users' demand responses. To present the flexibility of PEVs recharging load, we model it as a statistical random variable with a certain probability distribution. Two quantitative risk measures are defined to represent both the cost magnitude and economic uncertainties that PEVs recharging load could bring to the power systems. Then, a process integrated with PEV users demand response is developed to find the optimal electricity rate which provides the fair price for both power utilities and consumers, and has the lowest risk measures. Three types of rate mechanisms, flat rate, 3-steps TOU and 24-steps TOU rates, are examined particularly in the case study and their effectiveness are compared based on defined measurements.

The reminder of this paper is organized as follows: Section 2 defines two risk measures of PEVs recharging load based on the economic dispatch model. Section 3 presents the PEV users demand response model and the process of optimizing the electricity rate. Section 4 gives a case study based on a 10-bus system, and the effect of PEV users demand response model is examined. Section 5 is the conclusion.

4.2 Risk Measures of PEVs Recharging Load

In this paper, we use risk measures to evaluate the impact of PEVs recharging load on the power systems. The risk measures are defined in terms of two aspects. The first aspect is the magnitude of power systems' incremental cost due to PEVs recharging load. The second aspect is defined as the range of economic uncertainties that caused to the power systems by the PEVs recharging load. Both of these two risk measures will be presented in detail in the following sections.

4.2.1 Modeling of PEVs Recharging Load

The flexibility of PEVs' recharging load is an important feature which makes it different from baseline load. We use $d_{n,t}$ and $\Delta d_{n,t}$ to denote the baseline electric load and PEVs recharging load in location n at hour t, respectively. For a specific location and hour, the baseline load is assumed to be a fixed value. The way to model PEVs' recharging load is based on multinomial distributions, which is explained in details as follows.

It is assumed that each PEV needs Δt consecutive hours to recharge to fulfill their driven demand during time horizon $\mathbf{T} = \{1, 2, ..., T\}$. PEVs total recharging load at hour t in location n is denoted as $\Delta d_{n,t}$, which is contributed by all the PEVs that start to recharge at hours from $t - \Delta t + 1$ to t. We use $M_{n,t}$ to denote the number of PEVs that start to recharge from hour t in location n, then $\sum_{t=t-\Delta t+1}^{t} M_{n,t}$ shows the total number of PEVs that are recharging at hour t. Parameter f represents the efficiency of charging facilities, which transfers the number of recharging PEVs to electricity load. Thus, the recharging load $\Delta d_{n,t}$ could be calculated as:

$$\Delta d_{n,t} = f \times \sum_{t=t-\Delta t+1}^{t} M_{n,t}.$$

The vector $M_n = [M_{n,1}, M_{n,2}, ..., M_{n,T}]$ is used to represent the number of PEVs that

start to recharge in location n for all the hours $1, 2, ...T$, which is modeled as the following multinomial distribution. Parameter V_n denotes the total number of PEVs in location n, which is a fixed value. Vector $P_n^s = [p_{n,1}^s, p_{n,2}^s, ..., p_{n,T}^s]$ presents the probabilities of a PEV that starts to recharge in location n at hours $1, 2, ..., T$.

$$M_n \sim \text{Muln}(V_n, P_n^s), \forall n.$$

Vector $P_n^0 = [p_{n,1}^0, p_{n,2}^0, ..., p_{n,T}^0]$ denotes the recharging probabilities of a PEV in location n that is recharging at hours $1, 2, ..., T$. All the $p_{n,t}^0$ should be greater than 0 and satisfy $\sum_{t \in \mathbf{T}} p_{n,t}^0 = 1, \forall n$. PEV users make the recharging decisions according to the average recharging probability of the next Δt consecutive hours. Thus, the following equation shows the relationship between the recharging probability $p_{n,t}^0$ and $p_{n,t}^s$.

$$p_{n,t}^s = \sum_{t=t}^{t+\Delta t-1} p_{n,t}^0 / \Delta t.$$

In the later part of this paper, we use Δd_t to denote a set of random variables $\Delta d_{n,t}$ for all the locations $n \in \mathbf{N}$ at hour t, and Δd to denote the set of random variables $\Delta d_{n,t}$ for all the locations $n \in \mathbf{N}$ and hours $t \in \mathbf{T}$. Thus $\Delta d_t = \{\Delta d_{n,t} : n \in \mathbf{N}\}$ and $\Delta d = \{\Delta d_{n,t} : n \in \mathbf{N}, t \in \mathbf{T}\}$.

4.2.2 PEVs' Cost and Payment to the Power Systems

An economic dispatch model is applied to calculate the cost and payment of PEVs recharging load to the power system. The economic dispatch model is a classic optimization problem that is to obtain the optimal supply of electricity generators to meet the system load demand with the minimum generation cost. By solving the model, we can not only find the optimal electricity supply on each time and location, but also get the minimal total generation cost.

In the economic dispatch model, we separate the total electricity load into baseline load and PEVs recharging load. The two decision variables of the model are electricity supply $q_{n,t}$ and the load net injection $z_{n,t}$ on location n at hour t. Since we assume that baseline load is

fixed and recharging load is a random variable, the minimal generation cost from the model could be expressed as a function of recharging load, denoted as $\zeta_t(\Delta d_t)$.

The mathematical form of the economic dispatch model is presented as follows.

$$\min_{q_{n,t},z_{n,t}} \quad \zeta_t(\Delta d_t) = \sum_n (\tfrac{1}{2} a_{n,t} q_{n,t}^2 + b_{n,t} q_{n,t}) \tag{4.1}$$

$$\text{s.t.} \quad q_{n,t} - z_{n,t} = d_{n,t} + \Delta d_{n,t}, (p_{n,t}) \forall n, t \tag{4.2}$$

$$-T_l \leq \sum_n H_{n,t} z_{n,t} \leq T_l, \forall l, t \tag{4.3}$$

$$\sum_n z_{n,t} = 0, \forall t \tag{4.4}$$

$$0 \leq q_{n,t} \leq Q_{n,t}, \forall n, t \tag{4.5}$$

Where

- $\zeta_t(\Delta d_t)$: the total generation cost of the power systems to fulfill the baseline load and PEVs recharging load Δd_t;
- $q_{n,t}$: electricity generation (supply) in location n at hour t;
- $d_{n,t}$: baseline electric load in location n at hour t;
- $\Delta d_{n,t}$: PEV recharging load in location n at hour t;
- $z_{n,t}$: load net injection in location n at time t;
- $H_{l,n}$: power transfer distribution factor for transmission line l and location n;
- $Q_{n,t}$: generation capacity in location n at hour t;
- $p_{n,t}$: LMP in location n at hour t, which is the dual variable to the first set of constraints;
- $a_{n,t}, b_{n,t}$: cost generation parameters in location n at hour t.

The objective function (1) is to minimize the total generation cost given the parameters $a_{n,t}$ and $b_{n,t}$. The total electricity generations have to equal the system baseline load and the

PEV recharging load, which is shown in constraint (2). Constraints (3) and (5) are the transmission line capacity and generation capacity restrictions respectively. Constraint (4) means the total load net injection should equal 0. Locational marginal price (LMP) $p_{n,t}$ is defined as the generation cost to meet the next unit of load demand at a specific location n at hour t, which is the dual variable to constraint (2).

In this paper, PEVs' cost and payment are calculated using the economic dispatch model. On one hand, PEVs cost to the power systems can be treated as the incremental cost due to the PEVs recharging load. which is defined as the difference of the minimal costs between the economic dispatch models with and without the PEVs recharging load for all locations $n \in \mathbf{N}$ and hours $t \in \mathbf{T}$. The mathematical form is:

$$\delta(\Delta d) = \sum_{t \in \mathbf{T}} [\zeta_t(\Delta d_t) - \zeta_t(0)].$$

On the other hand, electric utilities impose recharging payment from PEV users at certain electricity rates. PEVs payment to the power systems is determined by recharging load allocation and electricity rate. We define $\eta(\Delta d, r)$ as PEV users' recharging payment to the power system for all locations $n \in \mathbf{N}$ and hours $t \in \mathbf{T}$, then

$$\eta(\Delta d, r) = \sum_{n \in \mathbf{N}, t \in \mathbf{T}} r_{n,t} \Delta d_{n,t}.$$

Here, $r_{n,t}$ is used to denote electricity rate in location n at hour t. r_n is the set of electricity rates of all hours $t \in \mathbf{T}$ in location n, and r is the set of electricity rates for all locations $n \in \mathbf{N}$ and hours $t \in \mathbf{T}$. Thus $r_n = \{r_{n,t} : t \in \mathbf{T}\}$ and $r = \{r_{n,t} : n \in \mathbf{N}, t \in \mathbf{T}\}$.

4.2.3 Risk Measures of PEVs Recharging Load

The flexibility of PEV users recharging behavior leads to randomness of both PEVs cost and payment to the power systems. For PEVs cost, recharging behavior happens during peak baseline load hours costs more than during off-peak load hours since higher cost generators need

to be used to fulfill additional load demand. For PEVs recharging payment, under flat electricity rate where prices are the same over time, PEV users' recharging payment keeps constant no matter when recharging behaviors take place. Under TOU rates where electricity rates are time dependent, recharging payment depends on PEV users' choice of recharging time periods. Recharging behavior during high electricity rate hours pays more than during low electricity rate hours.

Under a certain electricity rate, each realization of PEV users recharging behavior generates a specific case of PEVs payment and cost to the power system, which is shown in Figure 4.1 as a point in the payment-cost space. Under ideal electric rates, the payment from PEV users for electricity assumption should reflect the true energy cost to the power systems. In Figure 4.1, the points on the 45-degree line shows that PEV users pay as much as they cost to the power systems. If cost is greater than payment, the power system has a deficit; if cost is smaller than payment, the power system has a surplus.

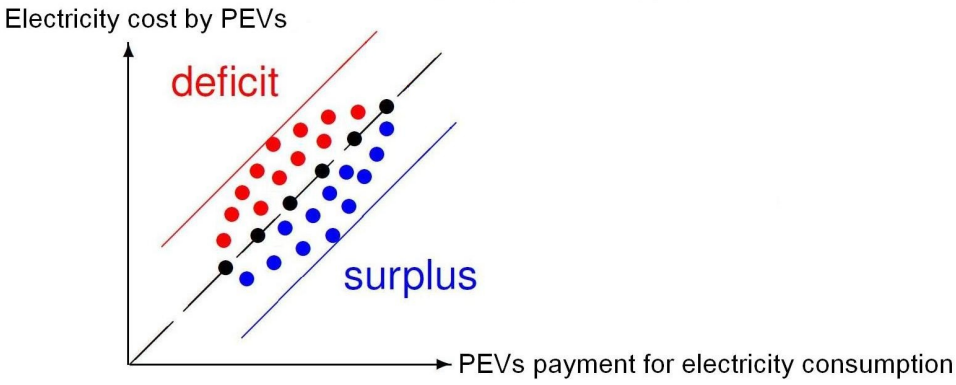

Figure 4.1 PEVs cost and payment to the power systems

The distributions of PEVs payment and cost to the power systems build an area in the payment-cost space, which is named as the risk measure area. The two risk measures are defined based on the characteristics of the risk measure area.

The first risk measure is used to represent the height of the risk measure area on the cost

axis, which shows the magnitudes of PEV cost to the power systems. Under fair condition when PEVs payment equals cost, this risk measure could also represent the PEVs payment to the power systems. Therefore, based on PEVs recharging load Δd, the first risk measure is defined as the expected cost of PEVs recharging load, whose mathematical form is shown as

$$\mathcal{M}_1(\Delta d) = \mathrm{E}(\delta(\Delta d)).$$

The second risk measure is used to represent the width of the risk measure area along the 135-degree direction, which shows the deficit and surplus range that PEVs could bring to the power systems. The larger width means PEVs recharging load poses more economic uncertainties while a thinner area means PEV users recharging behavior follows a more certain pattern. We define $\mathcal{D}(r, \Delta d)$ as the difference between PEVs payment and cost to the power system given electricity rate r, shown as $\mathcal{D}(r, \Delta d) = \delta(\Delta d) - \eta(\Delta d, r)$. Since $\Delta d_{n,t}$ is a random variable, $\mathcal{D}(r, \Delta d)$ is also a random variable with a certain distribution. Based on the distribution of random variable $\mathcal{D}(r)$, we define the second risk measure of PEVs recharging load as:

$$\mathcal{M}_2(r, \Delta d, \alpha_1, \alpha_2) = \mathrm{VaR}_{\alpha_1}(\mathcal{D}(r, \Delta d)) - \mathrm{VaR}_{\alpha_2}(\mathcal{D}(r, \Delta d)), \text{ for } 0 < \alpha_2 < \alpha_1 < 1.$$

Here, Value at Risk (VaR) is a widely used measure to estimate the value with a certain level of confidence. $\mathrm{VaR}_{\alpha_1}(\mathcal{D})$ ($\mathrm{VaR}_{\alpha_2}(\mathcal{D})$) denotes the threshold value such that the probability of $\mathcal{D}$ exceeding this value is the given probability α_1 (α_2). In this way, risk measure $\mathcal{M}_2(r, \Delta d, \alpha_1, \alpha_2)$ is defined as the inter-percentile range of the $\mathcal{D}$ distribution. There are two reasons of using inter-percentile range instead of using minimum to maximum range. Firstly, the extreme events happen with very small probability, which is not practical in real world. Secondly, the inter-percentile range is easier to estimate by Monte Carlo simulation, which is described in the next section. In this paper, α_1 is set to be 95%, and α_2 is set to be 5%.

4.2.4 Computation of Risk Measures

Monte Carlo simulation is a widely used technique in the probabilistic analysis of systems. It uses numerical experiments to obtain the statistics of output variables given the statistics of input variables. In this paper, we use Monte Carlo simulation to estimate the risk measures given the distribution of PEVs' recharging load.

We choose random samples from the multinomial distribution $\mathrm{Muln}(V_n, p_{n,t})$, plug into the economic dispatch model, calculate PEVs cost and payment to the power systems, and estimate the risk measures $\mathcal{M}_1$ and $\mathcal{M}_2$. The sample size is critical to the simulation results. According to the law of large numbers, the estimation obtained from a large size sample should be close to the expected value. Too few samples lead to inaccurate estimation while too many samples is time consuming. To obtain a good balance between time and accuracy, we perform a sensitivity analysis on the sample size, whose result is shown as in Figure 4.2. The estimations of risk measures become steady when the sample size is greater than 400.

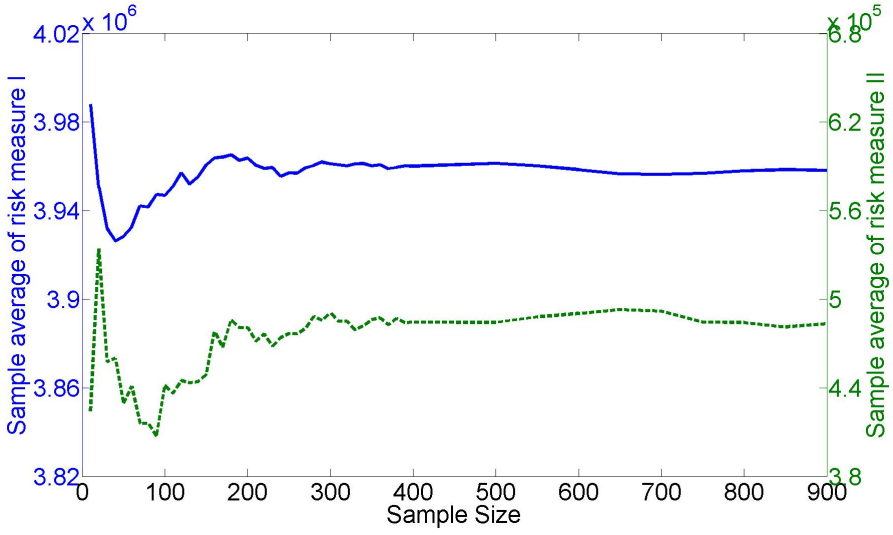

Figure 4.2 Sample size determination

4.3 The Optimal Electricity Rates

This section describes the demand response program and the process of optimizing the electricity rates to satisfy the fair price condition and have the lowest risk measures. We assume that the smart grid network could provide special recharging infrastructure for PEV load to have its separate electricity rate from baseline load. Under this assumption, the optimal electricity rate in this paper is only for PEVs recharging load.

4.3.1 PEV Users Recharging Demand Response Model

Power utilities provide TOU rates to encourage PEV users to shift some of their recharging demands from higher cost hours to lower cost hours. In this process, demand response model determines how sensible PEV users' behaviors are responsive to time dependent electricity rates. PEV users recharging behavior are mainly driven by two forces: convenience and cost. Under flat rate, PEV users behavior follows convenient recharging pattern. Under TOU rate, changes of recharging behavior happens based on the level of price incentives and consumers response sensitivity.

In this paper, demand response is defined as the changes in electric usage by PEV users from their convenient consumption patterns in response to changes in the electricity rates over time [5]. The following demand response model [13] is adopted to present the adjustment of PEVs recharging behavior in response to electric rates.

$$f(r) : \Delta P/P^0 = E \times \Delta R/R^0.$$

Here, vector $R^0 = [R_1^0, R_2^0, ..., R_T^0]'$ denotes the initial electricity rates for all the hours $1, 2, ..., T$; Vector $\Delta R = [\Delta R_1, \Delta R_2, ..., \Delta R_T]'$ means the changes of electricity rates from the initial electricity rates R^0; Vector $P^0 = [p_1^0, p_2^0, ..., p_T^0]'$ denotes the initla recharging probability; Vector $\Delta P = [\Delta p_1, \Delta p_2, ..., \Delta p_T]'$ denotes the responsive changes in the PEVs charging probability from the initial probability P^0; Parameter E is the elasticity matrix that presents the price elasticity of charging probability, which indicates the relative change in recharging demand

results from a change in the electricity price. The diagonal elements of the matrix present the self-elasticities and the off-diagonal elements present the cross-elasticities. Column j in matrix E indicates how a change in price during the time period j affects the recharging probability during all the periods.

4.3.2 Definition of the optimal electricity rate

Together with demand response program, electricity rate is an effective tool on mitigating PEVs impact. By optimizing electricity rates, power utilities are capable of regulating PEV users recharging behaviors and further reducing power systems generation cost to fulfill PEVs recharging load demand.

In this paper, the optimal electricity rate are defined from two aspects. Firstly, it should satisfy the following fair price condition; secondly, it should have the lowest risk measures.

Fair price condition: Given a K-steps electricity rate, the time period for each step is denoted as $\mathbf{T}_k$, $k = 1, 2, ...K$. For each time period of price step T_k, electricity rate should make the PEVs' expected payment equal to their expected cost to the power systems, whose mathematical form is shown as follows:

$$E(\sum_{t\in\mathbf{T}_k}(\zeta_t(\Delta d_t) - \zeta_t(0))) = E(\sum_{t\in\mathbf{T}_k} r_t \Delta d_t), \forall k = 1, 2, ..., K.$$

The fair price condition provides fairness not only between power utilities and PEV users, but also among different PEV users. For the former case, this condition makes sure that the power utilities collect as much payment as its generation cost to fulfill PEVs recharging load, and PEV users' payment equals to their cost to the power systems. For the latter case, this condition makes sure that for each particular recharging time period, PEV users pay as much as they cost to the power system.

Our study shows that risk measures are mainly different over different electricity rate mechanisms. Within the same rate plan, e.g., 3-steps TOU rate with determined time periods of price step, the level of electricity prices has limited impact on the risk measures. Risk measures only have significant improvement when the number of electricity rate or the time periods of price steps are changed. Thus, for each given setup of electricity rates, we could find an electricity price that satisfies the fair price condition, which is called optimal electricity rate under a certain type of rate mechanism or sub-optimal electricity rate. Among all the sub-optimal electricity rates, the optimal electricity rate is the one that has the lowest risk measures.

4.3.3 Electricity rates mechanisms

In this paper, three types of electricity rates mechanisms, flat rate, 3-steps TOU rates, and 24-steps TOU rates, are studied and their effectiveness on mitigating PEVs impact are examined. The more price steps electricity rates have, the more granularity and control ability it has on PEVs recharging behavior. Within each price step, electricity rate has no influence on PEV users recharging behavior.

Under flat rate, electricity prices are the same across time. In this case, convenience is the only issue that PEV users consider for their choice of recharging time periods. A single level electricity rate has a linear effect on the PEVs payment to the power system, but it has no influence on PEV users' recharging behavior. Thus, the price level is the only decision variable and the optimal flat rate is the one which makes PEV users' payment equal to the expected cost of recharging load.

TOU rate divides the entire time horizon (24 hours) into multiple time periods with different rates. Under TOU rates, recharging payment becomes an important consideration for PEV users besides of their convenience. Price incentives stimulate a certain amount of recharging load to shift from high-rate time period to low-rate time period. The number of TOU rate steps, the time period of each step, and the electricity rate for each step all influence PEV

users recharging behaviors.

In this paper, flat rate, 3-steps and 24-steps TOU rates are designed separately and their efficiencies are compared. For flat rate, the single level price is optimized. For 3-steps TOU rate, choice of time periods and electricity rate for each step are both optimized. For 24-steps TOU rate, the optimal electricity price for each hour is achieved.

4.3.4 Process of Finding the Optimal Electricity Rate

As stated previously, the optimal electricity rate needs to satisfy the fair price condition and have lowest risk measures. Our study shows that risk measures are mainly different over different rate mechanisms. Thus, the process of finding the optimal electricity rate is firstly find sub-optimal electricity rate under each of the three electricity rate mechanisms, then use Monte Carlo simulation method to obtain the risk measures corresponding to each electricity rate, and finally compare these risk measures to find the overall optimal electricity rate.

For each electricity rate mechanism, we use the following process to find the sub-optimal electricity price that satisfies the fair price condition. The process is also shown in Figure 4.3.

- Step 0: Setup an initial electricity rate and PEVs recharging load distribution;
- Step 1: Compute PEVs cost and payment to the power systems for each hour. Check whether PEVs cost equals payment for each time period of rate step. If it is equal, stop and obtain the electricity rate; otherwise goes to step 2;
- Step 2: Improve the electricity rate;
- Step 3: For the improved rates, update the PEVs recharging behavior according to PEVs demand response model. Step goes back to Step 1.

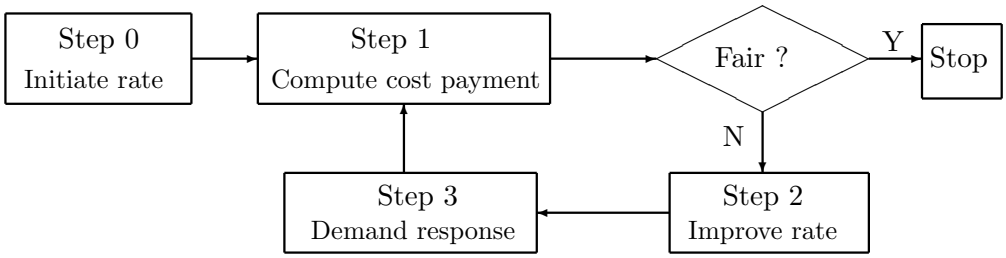

Figure 4.3 Process of finding the sub-optimal electricity rates

4.4 Case Study

A case study is conducted with a 10-bus system, which has 10 generators, 10 loads, and 12 transmission lines. The average electricity load per location over a one-year horizon is 328.56 MW, which is treated as baseline load. We make the following assumptions on PEVs recharging load.

- The number of PEVs in each location is assumed to be 1000.
- All the recharging infrastructures are using equipment with a 240 VAC, 40 Amp branch circuit, which is referred as the primary method for PEV recharging that can be performed in both private and public locations [14]. Under the provided charging power of 9.6 KW, PEVs can pose 9600 KW loads to each location if they charge at the same time, which is about 3% of average baseline load.
- Every PEV is recharged for 6 consecutive hours per day. Taking Chevy Volt as an example, the vehicle battery needs 4 hours to be fully recharged under assumed recharging infrastructure [1], which can provide a 38 miles all-electric range. With 53 miles daily average driving need [2], it needs 1.5 times of recharging per day on average, which is 6 hours.
- PEVs initial recharging probability is set as convenient recharging probability under flat

rate, whose curve follows the same curve pattern of average percentage of vehicles parked anywhere [24], shown as in Figure 4.4.

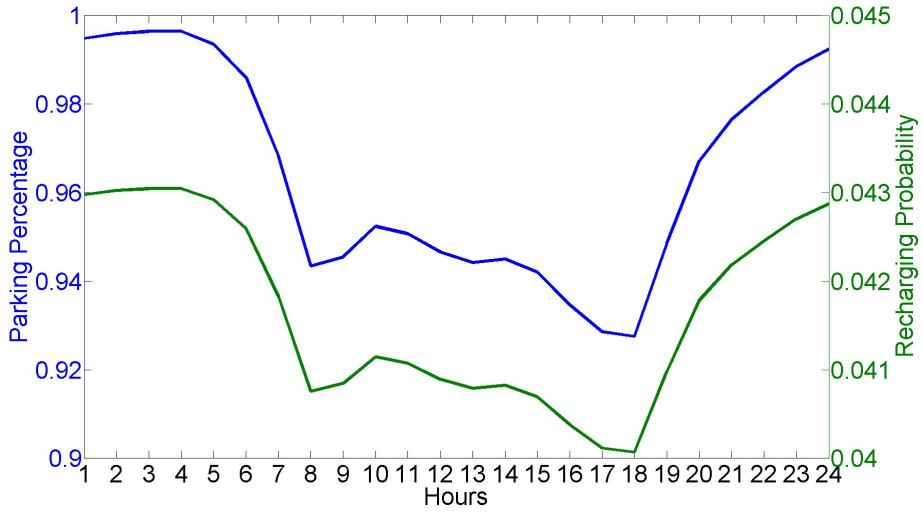

Figure 4.4 Convenient recharging probability

- For the demand response model, the elasticity matrix E is assumed to have the following formation. The self-elasticities are set to be $-e$, and the off-diagonal is set to be $e/23$. e is named as elasticity factor and the default value is set to be 1. This setup means that 1% increase in electricity rate will lead to 1% decrease of recharging probability for that hour, and the decreased recharging load switches equally to the other 23 hours in order to maintain the total recharging demand constant.

$$E = \begin{bmatrix} -e & e/23 & \cdots & e/23 \\ e/23 & -e & \ddots & \vdots \\ \vdots & \ddots & \ddots & e/23 \\ e/23 & \cdots & e/23 & -e \end{bmatrix}$$

We investigate the impact of PEV recharging with two scenarios and three types of electricity rates mechanisms. Scenario I assumes the electricity rates are the same across different locations. Scenario II assumes the rates can be different over locations. Under each scenario, flat rate, 3-steps TOU rate, and 24-steps TOU rate are optimized and the corresponding risk measures of PEV recharging load are compared.

4.4.1 Result I: Design of the Optimal Electricity Rates

We ran the 10-bus system with 365 days and conducted the simulation with 400 iterations to obtain yearly risk measures.

Table 4.1 lists the two risk measures for sub-optimal electricity rates under two scenarios and different electricity rate mechanisms. For the 3-steps TOU rate, different choices of price steps lead to different sub-optimal electricity prices. The best 3-steps TOU rates is the one that gives the lowest risk measures. In our case study, the best price steps for 3-steps TOU are 9-14, 15-23, and 24-8. For comparison purpose, the result of a non-best 3-steps TOU rate is also listed, which has price steps of hours 5-11, 12-19, and 20-4.

In both scenarios, the two risk measures are improved under the electricity rates with more price steps. Comparing 3-steps and 24-steps TOU rates with flat rate, we find that the price incentives encourage a certain amount of recharging load to switch from peak load hours to off peak load hours. Thus, for risk measure I, the PEVs expected cost to the power systems gradually decreases since less expensive generators are used to fulfill the load during off-peak load hours. The magnitude of reduced cost depends on multiple factors, including generation cost differences among generators, TOU rates, and PEV users' price responsiveness. This effect can be also shown in Figure 4.5, where the cost axis of the risk measure areas become lower comparing plots from left to right.

For risk measure II in both scenarios, there are also significant improvements by implementing electricity rate with more price steps. In scenario I, comparing with flat rate, risk measure II under the best 3-steps TOU improves by 61.5%. From the best 3-step TOU to 24-steps TOU, it improves by 12.2%. For scenario II, the improvements are 79.8% and 85.2% from flat rate to the best 3-steps TOU and further to 24-steps TOU rate, respectively. Same conclusion can be obtained from Figure 4.5, where the risk measure areas are thinner along the 135-degree direction under TOU rates with more price steps. Therefore, TOU rates can effectively reduce

Table 4.1 Risk measures under two scenarios

Scenario I	Flat rate	Non-best 3-steps TOU	Best 3-steps TOU	24-steps TOU
Risk Measure I ($\times 10^6$\$)	3.7716	3.6857	3.6250	3.6013
Risk Measure II ($\times 10^5$\$)	3.5231	2.5736	1.3569	1.1916
Scenario II	Flat rate	Non-best 3-steps TOU	Best 3-steps TOU	24-steps TOU
Risk Measure I ($\times 10^6$\$)	3.7716	3.6821	3.6203	3.5979
Risk Measure II ($\times 10^5$\$)	3.5029	2.4018	0.7093	0.1050

power system's economic uncertainty caused by PEV fleet.

From the comparison between the two scenarios, we can find scenario II has better performances than scenario I in terms of both risk measures. By allowing different electricity rates over locations, PEVs cost to the power systems, reflected in risk measure I, is reduced by a small amount while economic uncertainties, reflected in risk measure II, shows a relatively large improvement. Especially when the best 3-steps TOU and 24-steps TOU are used, risk measure II are improved by 47.7% and 91.2% comparing scenario II with scenario I, respectively. Therefore, PEVs economic uncertainties can be effectively reduced by bring more flexibility on electricity rates over locations.

4.4.2 Result II: Sensitivity Analysis of PEV Users' Recharging Behavior

Demand response to TOU rate is critical to the efficient management of PEVs recharging load. Many studies use survey and experimental methods to quantify the true magnitude of price elasticity. He et al. [11] obtained the demand responsiveness to four TOU rate designs based on the survey data collected in 2011 from 236 residents in China. It shows that the peak demand responsiveness are 8.41% and 21.26% when the peak-time prices increase by 20% and 40%, respectively. Vassileva et al. [21] found the response rates by sending a questionnaire to 2000 Swedish households. Although survey method reflects real responsiveness, uncertainties and bias may be included in the data collection and the results may not be general elsewhere.

In this paper, we conducted a sensitivity analysis to show the effect of price sensitivity of

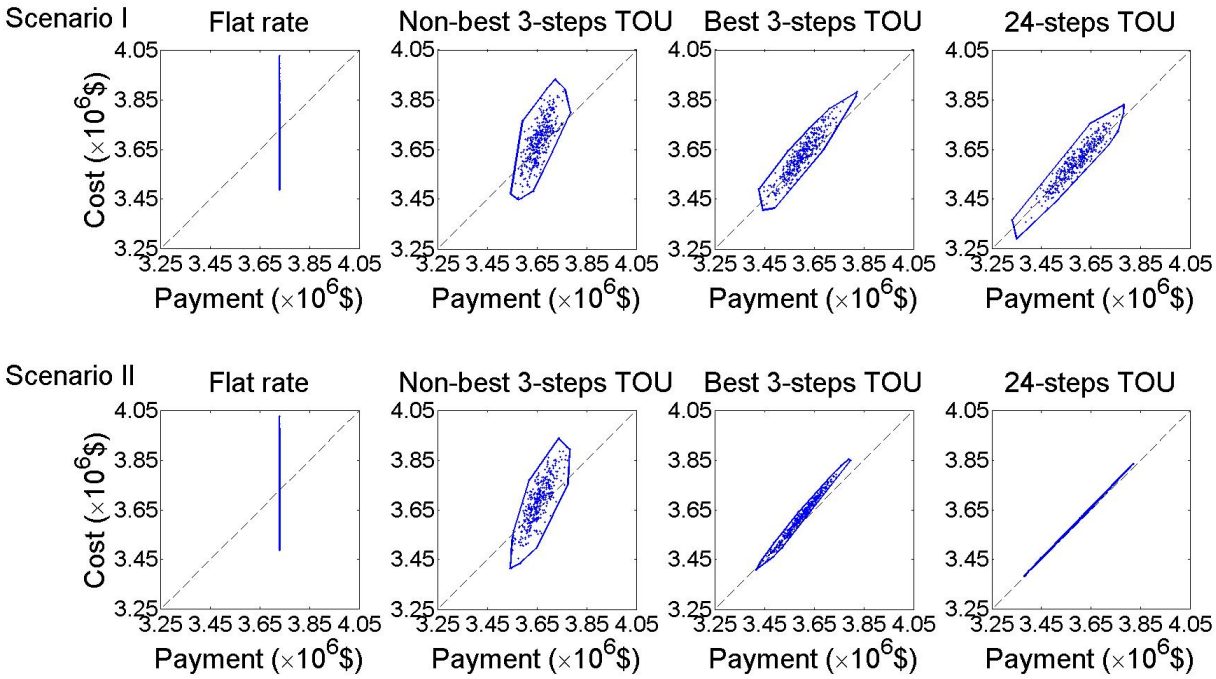

Figure 4.5 Risk measures for two scenarios under different electricity rate mechanisms

Table 4.2 Sensitivity analysis

	$e = 0.1$	$e = 1.0$	$e = 2.0$	$e = 3.0$
Risk Measure I ($\times 10^6$\$)	3.7577	3.6250	3.4920	3.3603
Risk Measure II ($\times 10^5$\$)	1.4599	1.3569	1.3294	1.1880

PEV users' responsiveness on the two risk measures. In the recharging demand response model, elasticity matrix presents how PEVs recharging behavior responses to electricity rates. In the sensitivity analysis, the same formation of elasticity matrix as in the previous case study is used.

We take the best 3-steps TOU rate under scenario I as an example. Four levels of elasticity factors, $e = 0.1$, $e = 1.0$, $e = 2.0$, and $e = 3.0$, are examined. They indicate that the decreased percentages of recharging probability corresponding to a Δ percentage increase of electricity rate are $0.1 \times \Delta$, $1 \times \Delta$, $2 \times \Delta$, and $3 \times \Delta$, respectively. Higher elasticity factor means PEV users recharging behavior is more sensitive to electricity rate changes.

Table 4.2 and Figure 4.6 show the risk measures under the four different elasticity factors.

The two risk measures gradually improve from the case with lowest elasticity factor to the case with the highest elasticity factor. The overall improvements are 10.6% and 18.6% for risk measure I and II, respectively. This shows that PEVs cost, payment, and economic uncertainties to the power systems all keep decreasing with higher recharging responsiveness.

Figure 4.7 shows the optimal 3-steps electricity rates and the corresponding recharging probability curves under the four elasticity factors. In the case with the highest elasticity factor (shown as green), even the electricity price difference between peak and off-peak load hours is low, more peak recharging load are triggered to switch from peak load hours to off-peak load hours due to more sensible recharging behavior, and this improves both risk measures shown in Table 4.2.

Therefore, high recharging responsiveness increases the effectiveness of price incentives and the control ability of power utilities under all scenarios and TOU rate mechanisms. From PEVs cost, payment and economic uncertainty perspectives, it is beneficial for both power systems and PEV users.

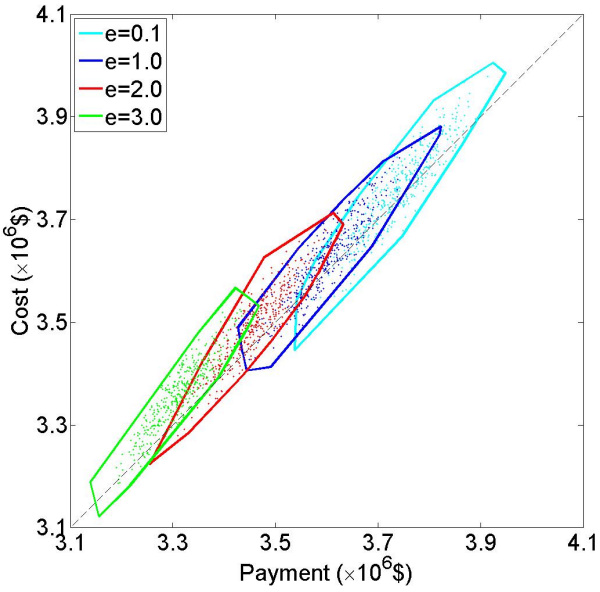

Figure 4.6 Risk measures under different elasticity factors

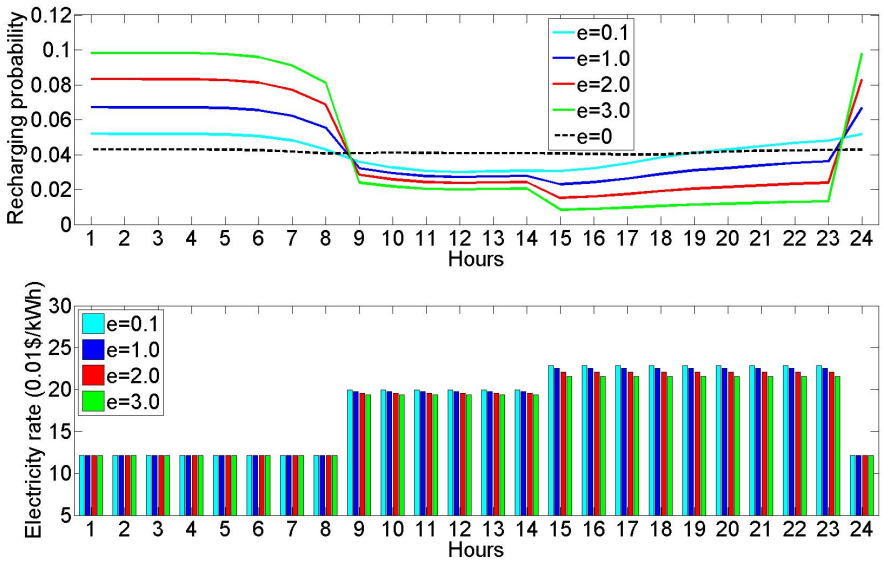

Figure 4.7 Recharging probability and the optimal electricity rate under different elasticity factors

4.5 Conclusion

Based on economic dispatch model, this paper defines two risk measures to assess the potential impact of PEVs recharging load on the power systems. These two assessments focus on the cost magnitude and the range of economic uncertainties that PEV fleet could bring to the power systems. Together with PEV users recharging demand response model and Monte Carlo simulation, a whole process is established to optimize electricity rates that could mitigate PEVs impact from the perspectives of defined risk measures. The sensitivity of PEV users demand response model is also studied.

The case study shows that properly designed 3-steps and 24-steps TOU rates can effectively regulate PEV users recharging behaviors and mitigate their effects to the power systems. Also, PEV users' high price responsiveness could effectively improve the control ability of power systems under TOU rates, which benefits both PEV users and the power systems. We believe that the model is general and important to the implementation of demand response program and design of electricity rates for the smart grid.

Future research directions include extending the design of electricity rates to dynamic pricing and real-time electricity rates, building more sophisticated demand response model with realistic survey data, and conducting case study with real world data.

Bibliography

[1] www.fueleconomy.gov.

[2] U.S. Department of Transportation. www.dot.gov.

[3] "Environmental assessment of plug-in hybrid electric vehicles. volume 1: Nationwide greenhouse gas emissions," Tech. Rep., EPRI, Palo Alto, CA. 1015325, 2007.

[4] "Plug-in hybrids: The next automotive revolution," Tech. Rep., Morgan Stanley, 2008.

[5] M. H. Albadi, and E. F. El-Saadany. "Demand response in electricity markets: An overview," *Power Engineering Society General Meeting, IEEE*, pp 1-5, 2007.

[6] P. Balducci, "Plug-in hybrid electric vehicle market penetration scenarios," Tech. Rep., Department of Energy, 2008.

[7] K. Clement-Nyns, E. Haesen, and J. Driesen, "The impact of charging plug-in hybrid electric vehicles on a residential distribution grid," *IEEE Transactions on Power Systems*, vol. 25, no. 1, pp. 371–380, 2010.

[8] P. Denholm and W. Short, "An evaluation of utility system impacts and benefits of optimally dispatched plug-in hybrid electric vehicles," Tech. Rep., National Renewable Energy Laboratory, 2006.

[9] Z. Duan, B. Gutierrez, and L. Wang. "Forecasting Plug-In Electric Vehicle Sales and the Diurnal Recharging Load Curve," *IEEE Transactions on Smart Grid*, vol. 5, no. 1, pp. 527-535, 2014.

[10] S. Hadley, "Evaluating the impact of plug-in hybrid electric vehicles on regional electricity supplies," *Bulk Power System Dynamics and Control-VII. Revitalizing Operational Reliability, iREP Symposium, IEEE*, pp. 1-12, 2007.

[11] Y. He, B. Wang, J. Wang, W. Xiong and T. Xia, "Residential demand response behavior analysis based on Monte Carlo simulation: The case of Yinchuan in China," *Energy*, 2012.

[12] I. Horowitz, and C. K. Woo, "Designing Pareto-superior demand-response rate options," *Energy*, vol. 31, no. 6, pp. 1040-1051, 2006.

[13] D. Kirschen, G. Strbac, P. Cumperayot, adn D. de Paiva Mendes, "Factoring the elasticity of demand in electricity prices," *IEEE Transactions on Power Systems*, vol. 15, no. 2, pp. 612-617, 2000.

[14] K. Morrow, D. Karner, and J. Francfort, "Plug-in hybrid electric vehicle charging infrastructure review," US Department of Energy-Vehicle Technologies Program, 2008.

[15] G. Putrus, P. Suwanapingkarl, D. Johnston, E. Bentley and M. Narayana, "Impact of electric vehicles on power distribution networks," *Vehicle Power and Propulsion Conference, VPPC'09, IEEE*, pp. 827-831, 2009.

[16] C. Roe, A. Meliopoulos, J. Meisel, and T. Overbye, "Power system level impacts of plug-in hybrid electric vehicles using simulation data," *Energy 2030 Conference, ENERGY, IEEE*, pp. 1-6, 2008.

[17] K. Schneider, C. Gerkensmeyer, M. Kintner-Meyer, and R. Fletcher, "Impact assessment of plug-in hybrid vehicles on pacific northwest distribution systems," *Power and Energy Society General Meeting-Conversion and Delivery of Electrical Energy in the 21st Century, IEEE*, pp. 1-6, 2008.

[18] S. Shao, T. Zhang, M. Pipattanasomporn, and S. Rahman, "Impact of TOU rates on distribution load shapes in a smart grid with PHEV penetration," *Transmission and Distribution Conference and Exposition, IEEE*, pp. 1-6, 2010.

[19] K. Sikes, T. Gross, Z. Lin, J. Sullivan, T. Cleary, and J. Ward, "Plug-in hybrid electric vehicle market introduction study: Final report," Tech. Rep., Oak Ridge National Laboratory (ORNL), 2010.

[20] Y. Strengers, "Air-conditioning Australian households: The impact of dynamic peak pricing," *Energy policy*, vol. 38, no. 11, pp.7312-7322, 2010.

[21] I. Vassileva, F. Wallin, and E. Dahlquist, "Understanding energy consumption behavior for future demand response strategy development," *Energy*, vol. 46, no. 1, pp. 94-100, 2012.

[22] R. Walawalkar, S. Fernands, N. Thakur, and K. Chevva, "Evolution and current status of demand response (DR) in electricity markets: insights from PJM and NYISO," *Energy*, vol. 35, no. 4, pp. 1553-1560, 2010.

[23] L. Wang, A. Lin, and Y. Chen, "Potential impacts of plug-in hybrid electric vehicles on locational marginal prices and emissions," *Naval Research Logistics*, vol. 57, no. 8, pp. 686–700, 2010.

[24] D. Wu, D. Aliprantis, and K. Gkritza, "Electric energy and power consumption by light-duty plug-in electric vehicles," *IEEE Transactions on Power Systems*, vol. 26, no. 2, pp. 738–746, 2011.

CHAPTER 5. CONTRIBUTION

The three papers in my thesis jointly study the optimization methodology and its applications in PEVs' potential impact on power systems. The first paper mainly focuses on the optimization theory, and the last two papers focus on the forecasting of PEVs' future development and their potential impact on power systems. The detailed conclusions and contributions of the three papers are discussed as follows.

The first paper presents heuristic algorithms for inverse mixed integer linear programming problems. The heuristic algorithms are designed to be implemented and executed in parallel with an existing algorithm in order to alleviate and overcome its two limitations. On one hand, it reduces the time and number of iterations for the existing algorithm to terminate; on the other hand, it also yields a series of improving feasible upper bound solutions that allow the tradeoff between reduced computation time and compromised solution quality. By using parallel techniques, we extend our problem solving ability and make the further efficiency improvement become possible.

In the second paper, we have presented two interactive models to jointly forecast PEV sales and the diurnal recharging load curve. Compared to existing approaches, our study makes the following new contributions. First, multiple factors are explicitly incorporated in the multiple linear regression model for PEV sales forecast. Second, we study decade-long historical data of HEV sales and other factors to extract information about how consumers make their vehicle purchasing decisions, which is utilized in the PEV sales forecast model. Third, we propose the convenience driven and cost driven modes to describe the transition of PEV users' recharging behaviors as a result of gradually prevailing smarter recharging infrastructures. Fourth, our

approach explicitly incorporates the interdependencies between sales forecast and recharging load forecast models.

In the third paper, we presented a model to access and mitigate PEVs' potential impact on the power systems. By designing different electricity rates plans, PEVs impact is minimized in terms of the two risk measures. Results show that TOU rates with more flexibilities have less PEVs recharging cost and uncertainties. PEVs responsiveness to the electricity rates is also studied and the sensitivity analysis in the case study shows that higher recharging responsiveness could improve the efficiency of the electricity rates. Optimization modeling, probability theories, and Monte Carlo Simulation are all used in this research. We believe the model established in this paper is general and a significant contribution to the research study and implementation of demand response program and design of electricity rates for the smart grid.

Our future work lies in the following directions.

As for the optimization theory, future research directions include designing more effective heristic algorithms for solving certain types of optimization problem. Extend the existing algorithm for single level optimization problem to bi-level and multiple level problem. On the implementation side, improve the communication efficiency of the auxiliary processors in the parallel implementation. Leverage existing parallel computing techniques in the resolution of the optimization problem.

For the PEVs sales forecasting, research extensions include surveying of early PEV users when sufficient samples are accessible to gather more valuable information for forecasting PEV penetration rates in future, exploring more advanced methodology and models to obtain more accurate prediction of PEVs sales, and investigating the viability of harnessing intermittent renewable energy to recharging PEVs.

For the topic of PEVs' potential impact on the power systems, a direct future research

is surveying of the PEV users recharging behaviors to get their real response pattern to the electricity rates, since their magnitude of responsiveness is the key factor that determines whether the way of designing electricity rates works or not. Moreover, conducting a larger case study with real world data would be a beneficial future work, which could be a indication of how valuable of studying PEVs' economic uncertainties to the power systems in the real world. At the same time, more advanced computing techniques, including parallel implementation of Monte Carlo Simulation, multi-level optimization models, could be applied in the extended future work.